

**NEW PHYSICS EFFECTS IN $B_c \rightarrow (D_s, D)\ell^+\ell^-$ DECAYS
IN SINGLE UNIVERSAL EXTRA DIMENSION**

**A THESIS SUBMITTED TO
THE GRADUATE SCHOOL OF NATURAL AND APPLIED SCIENCES
OF
KARABÜK UNIVERSITY**

BY

Elif DANAPINAR

**IN PARTIAL FULFILLMENT OF THE REQUIREMENTS
FOR
THE DEGREE OF MASTER OF SCIENCE
IN
DEPARTMENT OF PHYSICS**

July 2012

I certify that in my opinion the thesis submitted by Elif DANAPINAR titled “NEW PHYSICS EFFECTS IN $B_c \rightarrow (D_s, D)\ell^+\ell^-$ DECAYS IN SINGLE UNIVERSAL EXTRA DIMENSION” is fully adequate in scope and in quality as a thesis for the degree of Master of Science.

Assist. Prof. Dr. Ümit Oktay YILMAZ
Thesis Supervisor, Department of Physics



This thesis is accepted by the examining committee with a unanimous vote in the Department of Physics as a master thesis. June 21, 2012

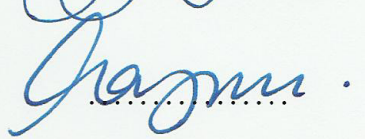
Examining Committee Members (Institutions)

Signature

Chairman : Assoc. Prof. Dr. Gökhan GÖKOĞLU (KBU)



Member : Assist. Prof. Dr. Nuray ER (AİBU)



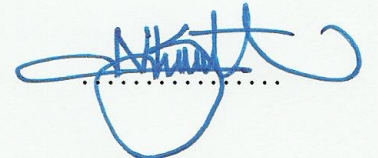
Member : Assist. Prof. Dr. Ümit Oktay YILMAZ (KBU)



....., 2012

The degree of Master of Science by the thesis submitted is approved by the Administrative Board of the Graduate School of Natural and Applied Sciences, Karabük University.

Prof. Dr. Nizamettin KAHRAMAN
Head of Graduate School of Natural and Applied Sciences



“I declare that all the information within this thesis has been gathered and presented in accordance with academic regulations and ethical principles and I have, according to the requirements of these regulations and principles, cited all those which do not originate in this work as well.”

Elif DANAPINAR

ABSTRACT

M.Sc. Thesis

NEW PHYSICS EFFECTS IN $B_c \rightarrow (D_s, D)\ell^+\ell^-$ DECAYS IN SINGLE UNIVERSAL EXTRA DIMENSION

Elif DANAPINAR

Karabük University

Graduate School of Natural and Applied Science

Department of Physics

Thesis Supervisor

Assist. Prof. Dr. Ümit Oktay YILMAZ

June 2012, 47 pages

The rare semileptonic $B_c \rightarrow D_{s,d}\ell^+\ell^-$ decays induced by flavor changing neutral currents are studied in the universal extra dimension with a single extra dimension scenario, in which the compactification radius R is the only new parameter. The sensitivity of differential and total branching ratio, and polarization asymmetries of final state leptons to the compactification parameter is presented, both for muon and tau decay channels. Comparing with the standard model, the obtained results indicate that there are new contributions to the physical observables. Considering the ability of available experiments, it would be useful to study these effects in searching new physics beyond the standard model.

Key Words : Flavor changing neutral current, semileptonic rare decay, universal extra dimension, the ACD model, lepton polarization.

Science Code : 202.1.149

ÖZET

Yüksek Lisans Tezi

TEK EVRENSEL FAZLA BOYUTTA $B_c \rightarrow (D_s, D)\ell^+\ell^-$ BOZUNUMLARINA YENİ FİZİK KATKILARI

Elif DANAPINAR

Karabük Üniversitesi

Fen Bilimleri Enstitüsü

Fizik Ana Bilim Dalı

Tez Danışmanı

Yrd. Doç. Dr. Ümit Oktay YILMAZ

Haziran 2012, 47 sayfa

Çeşni deęiřtiren yüksüz akımlarla gerekleřen nadir yarıleptonik $B_c \rightarrow D_{s,d}\ell^+\ell^-$ bozunumları, evrensel fazla boyutta, kompaktifikasyon yarıapının tek yeni deęiřken olduęu tek fazla boyut senaryosunda incelendi. Hem müon hem de tau bozunum kanalları için, diferansiyel ve toplam dallanma oranları ve son durumdaki leptonların polarizasyon asimetrilerinin kompaktifikasyon deęiřkenine duyarlılıęı sunuldu. Elde edilen sonuçlar, standart modelle karşılaştırıldığında, fiziksel gözlemlenebilirliğe yeni katkıların olduęunu göstermektedir. Var olan deneylerin donanımları düşünöldüğünde, bu katkıların incelenmesi standart model ötesi yeni fizik arařtırmalarında yararlı olacaktır.

Anahtar Sözcükler : Çeşni deęiřtiren yüksüz akımlar, yarıleptonik nadir bozunumlar, evrensel fazla boyut, ACD model, lepton polarizasyonu.

Bilim Kodu : 202.1.149

ACKNOWLEDGMENTS

First of all, I would like to express my sincere gratitude to my supervisor Assist. Prof. Dr. Ümit Oktay YILMAZ, not only for his guidance, encouragement, invaluable comments, patience and friendly attitude throughout all stages of my thesis but also for accepting me as a M.Sc. student. I also cannot express my appreciation to him for the time he spent to edit my thesis.

I am thankful to Res. Assist. Ulvi KANBUR for his help and advise about Computer tricks. I am also grateful to Müjgan ERGÜL YILMAZ for her help, support and friendly attitude. She has always been with me during the hard times.

Finally, there are no words to describe the appreciation and gratitude I feel for my family. I am proud to have such a family which gave me valuable advice and support when I needed it most. I know that I will never be able to thank them enough. And special thanks to my brother Ümit DANAPINAR for his invaluable support and encouragement during all my life.

CONTENTS

	<u>Page</u>
APPROVAL	ii
ABSTRACT	iv
ÖZET	v
ACKNOWLEDGMENTS	vi
CONTENTS	vii
LIST OF FIGURES	ix
LIST OF TABLES	xi
SYMBOLS AND ABBREVIATIONS INDEX	xii
CHAPTER 1	1
INTRODUCTION	1
CHAPTER 2	5
RARE DECAYS AND UNIVERSAL EXTRA DIMENSIONS	5
2.1. THE SM AND RARE B MESON DECAYS	5
2.2. THE EFFECTIVE HAMILTONIAN THEORY	8
2.3. UED AND THE ACD MODEL	14
CHAPTER 3	20
ANALYSIS OF $B_c \rightarrow (D_s, D)\ell^+\ell^-$ DECAYS IN THE ACD MODEL	20
3.1. EFFECTIVE HAMILTONIAN AND WILSON COEFFICIENTS	22
3.2. MATRIX ELEMENTS AND DECAY RATE	24
CHAPTER 4	31
LEPTON POLARIZATIONS IN $B_c \rightarrow (D_s, D)\ell^+\ell^-$ DECAYS	31
4.1. LEPTON POLARIZATION ASYMMETRY	31
4.2. ANALYSIS OF LEPTON POLARIZATION	35

	<u>Page</u>
CHAPTER 5.....	39
CONCLUSION.....	39
REFERENCES	41
APPENDIX A. INPUT PARAMETERS	45
AUTOBIOGRAPHY	47

LIST OF FIGURES

	<u>Page</u>
Figure 3.1. The variation of the Wilson coefficients with respect to $1/R$ at $q^2 = 14 \text{ GeV}^2$ for the normalization scale $\mu = 4.8 \text{ GeV}$	23
Figure 3.2. The dependence of differential branching ratio on s without resonance contributions for $B_c \rightarrow D_s \ell^+ \ell^-$. (In the legend $1/R = 200, 350, 500 \text{ GeV}$.)	26
Figure 3.3. The dependence of differential branching ratio on s without resonance contributions for $B_c \rightarrow D \ell^+ \ell^-$	26
Figure 3.4. The dependence of differential branching ratio on s with resonance contributions for $B_c \rightarrow D_s \ell^+ \ell^-$	28
Figure 3.5. The dependence of differential branching ratio on s without resonance contributions for $B_c \rightarrow D \ell^+ \ell^-$	28
Figure 3.6. The dependence of branching ratio on $1/R$ with and without resonance contributions for $B_c \rightarrow D_s \ell^+ \ell^-$	29
Figure 3.7. The dependence of branching ratio on $1/R$ with and without resonance contributions for $B_c \rightarrow D \ell^+ \ell^-$	29
Figure 4.1. The dependence of longitudinal polarization on s without resonance contributions for $B_c \rightarrow D_s \ell^+ \ell^-$	33
Figure 4.2. The dependence of longitudinal polarization on s without resonance contributions for $B_c \rightarrow D \ell^+ \ell^-$	33
Figure 4.3. The dependence of longitudinal polarization on s with resonance contributions for $B_c \rightarrow D_s \ell^+ \ell^-$	34
Figure 4.4. The dependence of longitudinal polarization on s with resonance contributions for $B_c \rightarrow D \ell^+ \ell^-$	34
Figure 4.5. The dependence of longitudinal polarization on $1/R$ with resonance contributions for $B_c \rightarrow D \ell^+ \ell^-$	35
Figure 4.6. The dependence of longitudinal polarization on $1/R$ with resonance contributions for $B_c \rightarrow D \ell^+ \ell^-$	35
Figure 4.7. The dependence of transverse polarization on s without resonance contributions for $B_c \rightarrow D_s \ell^+ \ell^-$	36
Figure 4.8. The dependence of transverse polarization on s without resonance contributions for $B_c \rightarrow D \ell^+ \ell^-$	36
Figure 4.9. The dependence of transverse polarization on s with resonance contributions for $B_c \rightarrow D_s \ell^+ \ell^-$	37

	<u>Page</u>
Figure 4.10. The dependence of transverse polarization on s with resonance contributions for $B_c \rightarrow D\ell^+\ell^-$	37
Figure 4.11. The dependence of transverse polarization on $1/R$ with resonance contributions for $B_c \rightarrow D_s\ell^+\ell^-$	38
Figure 4.12. The dependence of transverse polarization on $1/R$ with resonance contributions for $B_c \rightarrow D\ell^+\ell^-$	38

LIST OF TABLES

	<u>Page</u>
Table 2.1. The leptons and their fundamental properties.	6
Table 2.2. The quarks and their fundamental properties.	7
Table 2.3. Properties of the mediators and the force strengths.	7
Table 2.4. Charmonium ($\bar{c}c$) masses and widths.	14
Table 3.1. $B_c \rightarrow D_{s,d}$ form factors calculated in the constitute quark model.	27

SYMBOLS AND ABBREVIATIONS INDEX

ABBREVIATIONS

ACD	: Appelquist-Cheng-Dobrescu
ATLAS	: A Toroidal LHC Apparatus
CDF	: The Collider Detector at Fermilab
CKM	: Cabibbo-Kobayashi-Maskawa
CMS	: The Compact Muon Solenoid
CP	: Charge-Parity
FCNC	: Flavor Changing Neutral Current
GIM	: Glashow-Iliopoulos Maiani
KK	: Kaluza-Klein
LHC	: Large Hadron Collider
LL	: Leading Logarithmic
NDR	: Navie Dimensional Regularization
NLL	: Next-To-Leading Logarithmic
OPE	: Operator Product Expansion
QCD	: Quantum ChromoDynamics
RGE	: Renormalization Group Equation
SM	: Standard Model
UED	: Universal Extra Dimension

CHAPTER 1

INTRODUCTION

The Standard Model (SM) of elementary particle physics [1] is a renormalizable relativistic quantum field theory based on non-Abelian gauge symmetry of the gauge group $SU(3)_C \times SU(2)_L \times U(1)_Y$. The model allows us to understand the weak, electromagnetic and strong interactions in the last few decades. In spite of some conceptual problems, such as the number free parameters, the origin of mass, the hierarchy problem and etc., it has successfully explained phenomenology of particle physics and all experiments confirm the predictions within the experimental and theoretical uncertainty. Therefore, it is widely accepted that improvements in experiments and also theoretical developments, possible signals of new physics beyond the SM will most probably appear. In order to find satisfactory answers to the open questions of the SM some models which are extension of the SM, e.g. minimal supersymmetric model, two Higgs doublet model, left-right symmetric models, extra dimensions and etc., have been developed.

Rare B decays are special for providing important data in the structure of the SM and particle physics. By the word "rare", it is meant that c quark is not observed in the final states. These decays include the so called Cabibbo-suppressed decays and flavor changing neutral current (FCNC) decays, i.e. the decays occur via the current that change the flavor but not the charge of the quark. In the SM, the neutral currents are mediated through the gauge bosons Z_0, γ and g and do not change flavor. Therefore, these processes are absent in the SM at tree level, they occur at the loop level through the box and penguin diagrams. The loop effects are sensitive to the masses and other properties of the internal particles. Some other massive particles that are not available in the SM, such as fourth generation fermions, supersymmetric particles, may also give contributions to these decays.

Throughout the rare decays, the FCNC processes which occur at loop level in the SM provide us a powerful tool to test the SM and also a frame to study physics beyond the SM. After the observation of $b \rightarrow s\gamma$ by CLEO Collaboration [2], these transitions became more attractive and since this first observation rare radiative, leptonic and semileptonic decays of $B_{u,d,s}$ mesons have been intensively studied [3]. The experimental data for $B \rightarrow K^{(*)}\ell^+\ell^-$ also increased the interest on these decays. The experimental discovery of B_c meson, consists of b and c quarks, by The Collider Detector at Fermilab (CDF) Collaboration [4], opened a new area. The B physics studies will be more complete if similar studies for B_c meson are also included.

The study of B_c meson by itself is quite interesting, because of its outstanding features [5–7]. The B_c meson is the lowest bound state of two heavy quarks, a bottom-b and a charm-c quark, with explicit flavor. Comparing these with the $c\bar{c}$ -charmonium and the $b\bar{b}$ -bottomium bound states with implicit flavor, the latter decay strongly and electromagnetically, whereas the B_c decays weakly. Studying this meson in various decay channels are essential from both experimental and theoretical point of view. The B_c decays are attractive in determination of Cabibbo-Kobayashi-Maskawa (CKM) matrix elements V_{tq} ($q=b, s, d$), for checking the perturbative Quantum ChromoDynamics (QCD) and also they are very sensitive to the new physics, physics beyond the SM, because some new particles might give contributions in the loop diagrams.

On the experimental side of B_c decays, for example, at Large Hadron Collider (LHC), in pp collisions at $\sqrt{s} = 14$ TeV the $b\bar{b}$ cross section is expected to be $500 \mu b$. In a nominal year running will produce 10^{12} $b\bar{b}$ pairs, at the operational luminosity of $2 \times 10^{32} cm^{-2} sec^{-1}$, so with these facilities a complete spectrum of b hadrons including B_c will be accessible. A luminosity upgrade by a factor ten leads to collect an integrated luminosity of $100 fb^{-1}$. This upgrade will increase the leptonic data by a factor ten. At design luminosity, $10^{10} B_c$ events per year is estimated [8], this reasonable number is stimulating the work on the B_c phenomenology. At A Toroidal LHC Apparatus (ATLAS) and The Compact Muon Solenoid (CMS), most of the activities will be continued during the running luminosity of the order

$10^{32} - 10^{33} \text{cm}^{-2} \text{sec}^{-1}$ [9–11]. These possibilities will provide useful information on rare B_c decays as well as Charge-Parity (CP) violation and polarization asymmetries.

The B_c meson has radiative, leptonic and semileptonic decay channels. Throughout these decay modes, the semileptonic ones are especially interesting due to their relative cleanliness and sensitivity to new physics. In this thesis, we will study the new physics effects in the semileptonic rare $B_c \rightarrow (D_s, D)\ell^+\ell^-$ decays. In rare B meson decays, effects of the new physics may appear in two different ways; either through the new contributions to the Wilson coefficients existing in the SM or through the new structures in the effective Hamiltonian which are absent in the SM.

In rare decay calculations, the main tool is the effective Hamiltonian including the perturbative QCD corrections. The method begins with an operator product expansion (OPE) and performing a renormalization group equation (RGE) analysis and the heavy degrees of freedom are integrated out. As a result of this, one can parametrize the low energy weak processes in terms of perturbative short distance Wilson coefficients and long distance operator matrix elements; $H_{eff} \sim \sum C_i O_i$ [12–15].

Considering new physics beyond the SM, models including extra dimensions are particularly important because they include gravity and the other interactions, give hints on the hierarchy problem and a connection with string theory. Those with universal extra dimensions (UED) [16–19] have special interest because all the SM particles propagate in extra dimensions. Throughout the UED, a simpler scenario with a single universal extra dimension is the Appelquist-Cheng-Dobrescu (ACD) model [20]. The only additional free parameter with respect to the SM is the inverse of the compactification radius, $1/R$.

The main aim of this thesis is to find the effects of the ACD model on some physical observables related to the $B_c \rightarrow D_{q'}\ell^+\ell^-$ decays. Additionally, we give a SM analysis, by a couple of figures only. We study differential decay rate, branching ratio, and polarization of final state leptons, including resonance contributions in as many as possible cases. We analyze these observables in terms of the compactification factor

and the form factors. As an exclusive process, the theoretical calculation of the decays require the additional knowledge about these form factors which are the matrix elements of the Hamiltonian between the initial and the final state mesons. The form factors for $B_c \rightarrow D_{q'} \ell^+ \ell^-$ processes have been calculated using the quark models [21–24] and three-point QCD sum rules [26].

The thesis is organized as follows. In Chapter II, we give a brief summary on the SM and the rare decays. Also, we have briefly discussed the effective Hamiltonian theory and the ACD, including the modification of the Wilson coefficients. In Chapter III, we analyze the $B_c \rightarrow D_{q'} \ell^+ \ell^-$ decays, starting from the quark level processes $b \rightarrow (s, d) \ell^+ \ell^-$ and calculate the matrix element and the decay rate. The polarization asymmetries of the leptons are presented in Chapter IV and the last chapter is devoted to a summary and the conclusion of the thesis.

CHAPTER 2

RARE DECAYS AND UNIVERSAL EXTRA DIMENSIONS

Regarding the open questions in the Standard model and the physics beyond, many attempts have been done. The rare decays are one of the effective way to gather information both on the SM and new physics; the extensions of the SM and the models beyond the SM are other tools.

In this chapter, we will first review the Standard model and its situation and importance of rare B meson decays in particle physics. In the calculations we have used an effective theory in the heavy quark limit and here we will discuss how an effective Hamiltonian can be built up from a full theory and related Wilson coefficients. Additionally, the universal extra dimension and the ACD model is introduced with the modified Wilson coefficients.

2.1. THE SM AND RARE B MESON DECAYS

The Standard model is the unification of the electroweak theory and the quantum chromodynamics and describe the elementary particles and their interactions. The electroweak part of the model describes the electromagnetic and weak interactions of the quarks and leptons in $SU(2)_L \times U(1)_Y$ gauge symmetry where T and Y are weak isospin and hypercharge, respectively. The QCD is a vector gauge theory, $SU(3)_C$, describing the color interactions of quarks and gluons.

The quarks and the leptons together constitute the fermions and their properties are summarized in Table 2.1 and Table 2.2. In addition to the fermions there are bosons which are the mediators of the forces. The photon (γ) mediates the electromagnetic force, W^\pm and Z_0 correspond the mediation of weak force, and the gluons g mediate

the strong force, the properties of which are given in Table 2.3 with the force they carry and their strengths. Together with bosons, leptons and quarks are known as fundamental particles. Each particle in nature has an antiparticle with the same mass and spin but opposite charge. The strong force confine the quarks and make bound states. Those with a quark and an antiquark are called the mesons such as B_c^- which consists of $(b\bar{c})$ and bound of three quarks build up the baryons. In the SM, the interactions between the particles are described by gauge theories [27]. Although the

Table 2.1. The leptons and their fundamental properties.

Leptons (Spin=1/2)			
Particle Name	Symbol	Mass (GeV)	Charge
Electron	e	0.000511	-1
Electron neutrino	ν_e	$< 3 \times 10^{-9}$	0
Muon	μ	0.105	-1
Muon Neutrino	ν_μ	$< 1.9 \times 10^{-4}$	0
Tau	τ	1.77	-1
Tau Neutrino	ν_τ	1.82×10^{-2}	0

SM is a mathematically consistent renormalizable field theory which has successfully explained particles phenomenology and most of the experimental results, there are several unsatisfactory features. There are a lot of free physical parameters that can not be computed in the context of the SM. The Higgs sector of the theory remains unknown so far. The running experiments are expected to maintain useful information about Higgs and the mechanism. The neutrinos in the SM are massless. However, the experiments suggest nonzero masses. Gravity is not included in the SM, so it is not a complete theory of the nature. In the SM the only source of CP violation is the complex CKM matrix elements which appears too weak to derive the observed asymmetry in nature. There is also a "Hierarchy" Problem, the difference between the Planck scale ($10^{19} GeV$) and the electroweak scale ($100 GeV$ to $1 TeV$). These and many other unsatisfactory features of the SM and/or unanswered questions lead the physicists to search for new models beyond it. The phenomenology of the weak decays concern

Table 2.2. The quarks and their fundamental properties.

Quarks (Spin=1/2)			
Particle Name	Symbol	Mass (GeV)	Charge
Up	u		$2/3$
Down	d		$-1/3$
Charm	c		$2/3$
Strange	s		$-1/3$
Top	t		$2/3$
Bottom	b		$-1/3$

with all the unanswered questions of the SM summarized above is very rich of physics. Among the weak decays, the rare decays have a particular importance for providing the crucial information about the higher structure of the SM and also poorly studied aspects of it, particularly CKM matrix elements, the leptonic decay constants, and etc.

By rare decays, we generally mean decays which do not include a c quark into the

Table 2.3. Properties of the mediators and the force strengths.

Name	Mass (GeV)	Force Carried	Force Strength
g	0	<i>Strong</i>	10
γ	0	<i>Electromagnetic</i>	10^{-2}
W^\pm	80.40	<i>Weak</i>	10^{-13}
Z_0	91.18		
G	0	<i>Gravitation</i>	10^{-42}

final state and can be divided into two classes of transitions:

1. The quark level transitions due to the $b \rightarrow u$, which are suppressed relative to $b \rightarrow c$ modes by the CKM factor $|V_{ub}/V_{cb}| \approx 0.006$. These are called Cabibbo-suppressed decays. An example is the exclusive mode $B \rightarrow \rho \ell \nu$, with

a branching ratio of 2.5×10^{-4} .

2. A second class of rare decay modes is the transitions that are not available at the tree level in the SM. These transitions occur at loop level. Consequently, rare B decays, like ours, are mediated by FCNC processes of the kind $b \rightarrow s$ or $b \rightarrow d$.

The B meson systems have several features, which make them suitable, to study gauge structure of the SM and CP violation. In the loop diagrams, because of the top quark there is not GlashowIliopoulosMaiani (GIM) or CKM suppression, therefore, there are large CP violation effects and mixing possibilities. In addition, a variety of rare decays have larger branching ratios which allow us for detail studies. As a last remark, large b quark mass, which is greater than the scale of the strong interaction, provides less important long-distance strong interactions.

2.2. THE EFFECTIVE HAMILTONIAN THEORY

In theoretical rare decays we have to first calculate the transition amplitude between the initial B_c and final state (D_s, D) mesons. While doing this, all possible Feynman diagrams, which give contributions, are considered. The weak decays are mediated through weak interactions of quarks and the strong interactions of the quarks bind them into hadrons. As a result, the QCD effects must also be taken into account. At the level that is much smaller than $\hbar c/\Lambda_{QCD}$ the effects can be represented perturbatively by the exchanges of gluons. On the other hand, because of hadronization of quarks and gluons while moving of quarks over a distance of the order $\hbar c/\Lambda_{QCD}$, the QCD becomes nonperturbative. So, to understand the physics at different energy levels, different energy scales must be handled separately. The theoretical tool to evaluate the transition amplitude is the OPE [28].

In OPE, the transition amplitude \mathcal{M} for, in general, $B \rightarrow f$, where B and f represent the initial and final state mesons, respectively, can be written as

$$\mathcal{M} = \frac{G_F}{\sqrt{2}} \sum_i V_{CKM}^i C_i(\mu, m_{heavy}) \langle f | O_i(\mu) | B \rangle \left[1 + \mathcal{O}\left(\frac{m_b^2}{m_W^2}\right) \right]. \quad (2.1)$$

Here, O_i are the local operators and C_i are the Wilson coefficients. O_i and C_i depend on the QCD renormalization scale μ , and C_i depends on mass of the W boson and other heavy particles. In the expansion of the above equation, the non-perturbative QCD contributions are included in the operators while the perturbative effects manifest themselves in the Wilson coefficients. The operators do not depend on the large momentum scale of heavy particles. The Wilson coefficients are independent of the states f and B . Thus, different energy scales appear in this expansion. The renormalization scale μ satisfies the individual contributions. The way of choosing the μ scale is that the strong coupling constant should be low enough to make the perturbative calculations meaningful. In B meson decays, μ is usually taken as $\mathcal{O}(m_b)$, where m_b is the mass of b quark. The μ dependence in the operators $O_i(\mu)$ is canceled by that in the Wilson coefficients $C_i(\mu)$ because the physical amplitude can not depend on the scale.

A crucial properties of the method is the universality of the Wilson coefficients, i.e. their numerical values are the same for all final states f . Thus, C_i s can be considered as the effective coupling constant and the O_i s as the corresponding vertices. So, one can set up the effective Hamiltonian from the full theory as

$$\mathcal{M} = \frac{G_F}{\sqrt{2}} \sum_i V_{CKM}^i C_i(\mu, m_{heavy}) O_i(\mu) + h.c. . \quad (2.2)$$

Considering the unitarity of the CKM matrix, for $b \rightarrow s$ and the processes to build up an effective Hamiltonian, the effective Hamiltonian describing the semileptonic weak decays of B_c mesons in the quark level in the SM can be written explicitly in the following form

$$\mathcal{H}_{eff}(b \rightarrow s \ell^+ \ell^-) = -\frac{4 G_F}{\sqrt{2}} V_{tb} V_{ts}^* \sum_{i=1}^{10} C_i(\mu) O_i(\mu) , \quad (2.3)$$

where the operator basis is the same as in [15], and the operators are defined by

$$\begin{aligned}
\mathcal{O}_7 &= \frac{e}{16\pi^2} m_b (\bar{s}_L \sigma^{\mu\nu} b_R) F_{\mu\nu}, \\
\mathcal{O}_9 &= \frac{e^2}{16\pi^2} (\bar{s}_L \gamma_\mu b_L) (\bar{\ell} \gamma_\mu \ell), \\
\mathcal{O}_{10} &= \frac{e^2}{16\pi^2} (\bar{s}_L \gamma_\mu b_L) (\bar{\ell} \gamma_\mu \gamma_5 \ell).
\end{aligned} \tag{2.4}$$

Here, \mathcal{O}_7 is magnetic penguin operator, \mathcal{O}_9 and \mathcal{O}_{10} are semileptonic operators.

The coupling strength of the effective vertices O_i is given by the Wilson coefficients $C_i(\mu)$ and their values at large scale $\mu = \mu_W$ are obtained by matching the effective theory to the full one. In the SM, the $C_i(\mu_W)$ s are as follows [12–15]

$$\begin{aligned}
C_i(\mu_W) &= 0 (i = 1, 3, \dots, 6) \\
C_2(\mu_W) &= 1 \\
C_7(\mu_W) &= -\frac{1}{2} D'_0(x_t) \\
C_8(\mu_W) &= -\frac{1}{2} E'_0(x_t) \\
C_9(\mu_W) &= P_0^{NDR} + \frac{Y_0(x_t)}{\sin^2 \theta_W} - 4Z_0(x_t) + P_E E(x_t) \\
C_{10}(\mu_W) &= -\frac{Y_0(x_t)}{\sin^2 \theta_W}
\end{aligned} \tag{2.5}$$

with $x_t = m_t^2/m_W^2$ and

$$\begin{aligned}
D'_0(x_t) &= -\frac{(8x_t^3 + 5x_t^2 - 7x_t)}{12(1-x_t)^3} + \frac{x_t^2(2-3x_t)}{2(1-x_t)^4} \ln x_t \\
E'_0(x_t) &= -\frac{x_t(x_t^2 - 5x_t - 2)}{4(1-x_t)^3} + \frac{3x_t^2}{2(1-x_t)^4} \ln x_t \\
E(x_t) &= \frac{x_t(18 - 11x_t - x_t^2)}{12(1-x_t)^3} + \frac{x_t^2(15 - 16x_t + x_t^2)}{6(1-x_t)^4} \ln x_t - \frac{2}{3} \ln x_t \\
Y_0(x_t) &= \frac{x_t}{8} \left[\frac{x_t - 4}{x_t - 1} + \frac{3x_t}{(x_t - 1)^2} \ln x_t \right] \\
Z_0(x_t) &= \frac{18x_t^4 - 163x_t^3 + 259x_t^2 - 108x_t}{144(x_t - 1)^3} \\
&\quad + \left[\frac{32x_t^4 - 38x_t^3 - 15x_t^2 + 18x_t}{72(x_t - 1)^4} - \frac{1}{9} \right] \ln x_t. \tag{2.6}
\end{aligned}$$

The Wilson coefficients under QCD from a large scale, $\mu = \mu_W$ to a relevant scale for B decays, $\mu \approx m_b$, can be done perturbatively by applying the RGE

$$\mu \frac{d}{d\mu} C_i(\mu) = \sum_j \gamma_{ji} C_j(\mu). \tag{2.7}$$

γ in the above equation is the anomalous dimension matrix, which indicates that the operators mix under the renormalization. After the RGE evaluation steps, the $C_i(\mu)$ s can be decomposed into a leading logarithmic (LL), next-to-leading logarithmic (NLL) and next-next-to-leading logarithmic, etc., parts as

$$C_i(\mu) = C_i^{(0)}(\mu) + \frac{\alpha_s}{4\pi} C_i^{(1)}(\mu) + \frac{\alpha_s^2}{(4\pi)^2} C_i^{(2)}(\mu) + \mathcal{O}(\alpha_s^3). \tag{2.8}$$

The first term, $C_i^{(0)}(\mu)$, of the above equation gives the lowest order values, the LL parts, in the SM which are presented in Eq. (2.5). In the LL approximation, the Wilson coefficients for the operators O_1, \dots, O_7 are given by the following equations, where instead of C_7 a normalization scheme independent effective coefficient C_7^{eff} is

defined [12–15],

$$C_i(\mu) = \sum_j^8 k_{ij} \eta^{a_j} \quad (i = 1, \dots, 6),$$

$$C_7^{eff}(\mu) = \eta^{\frac{16}{23}} C_7^{(0)}(\mu_W) + \frac{8}{3} \left(\eta^{\frac{14}{23}} - \eta^{\frac{16}{23}} \right) C_8^{(0)}(\mu_W) + \sum_{j=1}^8 h_j \eta^{a_j} \quad (2.9)$$

with $\eta = \frac{\alpha_s(\mu_W)}{\alpha_s(\mu)}$, and

$$\alpha_s(x) = \frac{\alpha_s(m_Z)}{1 - \beta_0 \frac{\alpha_s(m_Z)}{2\pi} \ln\left(\frac{m_Z}{x}\right)} \quad (2.10)$$

where in fifth dimension $\alpha_s(m_Z) = 0.118$ and $\beta_0 = 23/3$. The numbers a_j , k_{ij} and h_j are given as

$$a_j = \left(\frac{14}{23}, \frac{16}{23}, \frac{6}{23}, -\frac{12}{23}, 0.4086, -0.4230, -0.8994, 0.1456 \right),$$

$$k_{1j} = \left(0, 0, \frac{1}{2}, -\frac{1}{2}, 0, 0, 0, 0 \right),$$

$$k_{2j} = \left(0, 0, \frac{1}{2}, \frac{1}{2}, 0, 0, 0, 0 \right),$$

$$k_{3j} = \left(0, 0, -\frac{1}{14}, \frac{1}{6}, 0.0510, -0.1403, -0.0113, 0.0054 \right),$$

$$k_{4j} = \left(0, 0, -\frac{1}{14}, -\frac{1}{6}, 0.0984, 0.1214, 0.0156, 0.0026 \right),$$

$$k_{5j} = \left(0, 0, 0, 0, -0.0397, 0.0117, -0.0025, 0.0304 \right),$$

$$k_{6j} = \left(0, 0, 0, 0, 0.0335, 0.0239, -0.0462, -0.0112 \right),$$

$$h_j = \left(2.2996, -1.088, -\frac{3}{7}, -\frac{1}{14}, -0.6494, -0.0380, -0.0186, -0.0057 \right). \quad (2.11)$$

Including the LL as well as NLL we define an effective coefficient, C_9^{eff} , which has

perturbative and resonance parts.

$$C_9^{eff}(s', \mu) = C_9(\mu) \left(1 + \frac{\alpha_s(\mu)}{\pi} w(s') \right) + Y(\mu) + C_9^{res}(\mu) \quad (2.12)$$

where $s' = q^2/m_b^2$ and

$$w(s') = -\frac{2}{9}\pi^2 - \frac{4}{3}Li_2(s') - \frac{2}{3}\ln s' \ln(1-s') - \frac{5+4s'}{3(1+2s')} \ln(1-s') \\ - \frac{2s'(1+s')(1-2s')}{3(1-s')^2(1+2s')} \ln s' + \frac{5+9s'-6s'^2}{6(1-s')(1+2s')}. \quad (2.13)$$

The perturbative part, coming from one-loop matrix elements of the four-quark operators, is

$$Y(\mu, s') = h(u, s') \left(3C_1(\mu) + C_2(\mu) + 3C_3(\mu) + C_4(\mu) + 3C_5(\mu) + C_6(\mu) \right) \\ - \frac{1}{2}h(0, s') \left(C_3(\mu) + 3C_4(\mu) \right) + \frac{2}{9} \left(3C_3(\mu) + C_4(\mu) + 3C_5(\mu) + C_6(\mu) \right) \\ - \frac{1}{2}h(1, s') \left(4C_3(\mu) + 4C_4(\mu) + 3C_5(\mu) + C_6(\mu) \right) \quad (2.14)$$

where

$$h(u, s') = -\frac{8}{9}\ln \frac{m_b}{\mu} - \frac{8}{9}\ln u + \frac{8}{27} + \frac{4}{9}x \\ - \frac{2}{9}(2+x)|1-x|^{1/2} \begin{cases} \left(\ln \left| \frac{\sqrt{1-x}+1}{\sqrt{1-x}-1} \right| - i\pi \right), & \text{for } x \equiv \frac{4u^2}{s} < 1 \\ 2 \arctan \frac{1}{\sqrt{x-1}}, & \text{for } x \equiv \frac{4u^2}{s} > 1, \end{cases} \\ h(0, s') = \frac{8}{27} - \frac{8}{9}\ln \frac{m_b}{\mu} - \frac{4}{9}\ln s + \frac{4}{9}i\pi, \quad (2.15)$$

with $u = m_c/m_b$.

The resonance contribution due to the conversion of the real $c\bar{c}$ into lepton pair can be done by using a Breit-Wigner formula as [29],

$$C_9^{res}(\mu, s') = -\frac{3}{\alpha_{em}^2} \kappa \sum_{V_i=J/\psi, \psi, \dots} \frac{\pi \Gamma(V_i \rightarrow \ell^+ \ell^-) m_{V_i}}{sm_b^2 - m_{V_i} + im_{V_i} \Gamma_{V_i}} \times \left[(3C_4(\mu) + C_2(\mu) + 3C_3(\mu) + C_4(\mu) + 3C_5(\mu) + C_6(\mu)) \right]. \quad (2.16)$$

The phenomenological parameter κ is taken 2.3 to produce the correct branching ratio $BR(B \rightarrow J/\psi K^* \rightarrow K^* \ell^+ \ell^-) = BR(B \rightarrow J/\psi K^*) B(J/\psi \rightarrow \ell^+ \ell^-)$ and the normalization is fixed by data given in [30]. There are six known resonances of $c\bar{c}$ that can contribute to the decay, the properties of which are summarized in Table 2.4.

We will not discuss the coefficient $C_8(\mu)$ here, which does not enter the Hamiltonian

Table 2.4. Charmonium ($\bar{c}c$) masses and widths.

Mesons	Mass(GeV)	$BR(V \rightarrow \ell^+ \ell^-)$	$\Gamma(GeV)$
$J/\Psi(1s)$	3.097	5.93×10^{-2}	92.9×10^{-6}
$\Psi(2s)$	3.686	7.70×10^{-3}	304×10^{-6}
$\Psi(3770)$	3.773	9.70×10^{-6}	27.3×10^{-3}
$\Psi(4040)$	4.039	1.70×10^{-5}	80×10^{-3}
$\Psi(4160)$	4.153	68.1×10^{-6}	103×10^{-3}
$\Psi(4415)$	4.421	9.40×10^{-6}	62×10^{-3}

for the $b \rightarrow s \ell^+ \ell^-$ decay, the analytic expression can be found in [13]. The Wilson coefficient C_{10} corresponding to \mathcal{O}_{10} is independent of scale μ since \mathcal{O}_{10} does not renormalize under QCD.

2.3. UED AND THE ACD MODEL

The SM of elementary particles has successfully passed several experimental tests, however, there are some unsatisfactory features of the theory. Also, most physicists agree that there must exist new physics beyond the SM, the nature of which is not yet known. With the aim of finding reasonable answers to the open questions of the SM

and catching clues for new physics, some extensions of the model, such as minimal supersymmetric model, two Higgs doublet model, left-right symmetric models, extra dimensions and etc. have been improved.

Among the proposed extensions of the SM, the models including extra dimensions have been widely taken into account [16–19, 31, 32]. Extra dimensions include gravity and other interactions, and also are considered to solve the hierarchy problem, gauge coupling unification and etc. Those with UED have special attraction because all the SM particles propagate in the extra dimensions. The extra dimensions are compactified and the compactification scale allows Kaluza-Klein (KK) partners of the SM fields in the four-dimensional theory and also KK excitations without corresponding SM partners.

Throughout the UED, a simpler scenario with a single universal extra dimension is the ACD model [20]. In this model the only additional free parameter with respect to the SM is the inverse of the compactification radius, $1/R$. In particle spectrum of the ACD model, there are infinite towers of KK modes ($n \geq 1$) and the ordinary SM particles are presented in the zero mode ($n = 0$). For each SM boson there is one such a tower, while two for each SM fermion. We have not introduced the field theoretical calculations for the extra dimensions but to convince the reader these can be found in details in [33–35]. The masses of the KK particles are universally given by

$$m_n^2 = m_0^2 + \frac{n^2}{R^2} \quad (2.17)$$

with m_0 , the mass of the zero mode. The KK modes contribute to the processes at the loop level so the variables in the $x(t) = m_t^2/m_W^2$ should be modified as

$$x_i(n) = \frac{m_i^2(n)}{m_W^2(n)} \quad (2.18)$$

where $m_i^2(n)$ and $m_W^2(n)$ are the masses of the fermionic and the W boson KK modes, respectively.

An important property of the ACD model is the conservation of the KK parity, which implies that the KK modes do not contribute at tree level for the low energy interaction processes and the lightest KK particle must be stable.

The new physics contributions in the ACD model appear by modifying available Wilson coefficients in the SM. The modified Wilson coefficients are calculated in [35, 36] and can be expressed in terms of $F(x_t, 1/R)$ which generalize the corresponding SM functions $F_0(x_t)$ according to

$$F(x_t, 1/R) = F_0(x_t) + \sum_{n=1}^{\infty} F_n(x_t, x_n) \quad (2.19)$$

with the mass of KK particles $m_n = n/R$, related to the Eq. (2.17). Here, $n = 0$ corresponds to the SM particles.

The effective, normalization scheme independent, coefficient $C_7^{eff}(\mu)$ defined in Eq. (2.9) can be modified in the leading logarithmic approximation defined as

$$C_7^{eff}(\mu_b, 1/R) = \eta^{16/23} C_7(\mu_W, 1/R) + \frac{8}{3} (\eta^{14/23} - \eta^{16/23}) C_8(\mu_W, 1/R) + C_2(\mu_W, 1/R) \sum_{i=1}^8 h_i \eta^{a_i}. \quad (2.20)$$

The functions in Eq. (2.20) are

$$C_2(\mu_W) = 1, \\ C_7(\mu_W, 1/R) = -\frac{1}{2} D'(x_t, 1/R), \quad C_8(\mu_W, 1/R) = -\frac{1}{2} E'(x_t, 1/R). \quad (2.21)$$

Here, $D'(x_t, 1/R)$ and $E'(x_t, 1/R)$ are defined by using Eq. (2.19) with the functions given in Eq. (2.6) and the followings

$$\begin{aligned}
D'_n(x_t, x_n) &= \frac{x_n(2 - 7x_n + 3x_n^2)}{6} \ln \frac{x_n}{1 + x_n} \\
&+ \frac{x_t(-37 + 44x_t + 17x_t^2 + 6x_n^2(10 - 9x_t + 3x_t^2) - 3x_n(21 - 54x_t + 17x_t^2))}{36(x_t - 1)^3} \\
&- \frac{(-2 + x_n + 3x_t)(x_t + 3x_t^2 + x_n^2(3 + x_t) - x_n(1 + (-10 + x_t)x_t))}{6(x_t - 1)^2} \\
&\times \ln \frac{x_n + x_t}{1 + x_n}, \tag{2.22}
\end{aligned}$$

$$\begin{aligned}
E'_n(x_t, x_n) &= \frac{x_t(-17 - 8x_t + x_t^2 - 3x_n(21 - 6x_t + x_t^2) - 6x_n^2(10 - 9x_t + 3x_t^2))}{12(x_t - 1)^3} \\
&+ \frac{(1 + x_n)(x_t + 3x_t^2 + x_n^2(3 + x_t) - x_n(1 + (-10 + x_t)x_t))}{2(x_t - 1)^4} \\
&- \ln \frac{x_n + x_t}{1 + x_n} \frac{1}{2} x_n(1 + x_n)(-1 + 3x_n) \ln \frac{x_n}{1 + x_n}. \tag{2.23}
\end{aligned}$$

The summations are carried out using the prescription defined in [35] or can be found in [37]. The expressions for the sum over n are

$$\begin{aligned}
\sum_{n=1}^{\infty} D'_n(x_t, x_n) &= -\frac{x_t(-37 + x_t(44 + 17x_t))}{72(x_t - 1)^3} \\
&+ \frac{\pi M_W R}{2} \left[\int_0^1 dy \frac{(2y^{1/2} + 7y^{3/2} + 3y^{5/2})}{6} \coth(\pi M_W R \sqrt{y}) \right. \\
&+ \frac{(-2 + 3x_t)x_t(1 + 3x_t)}{6(x_t - 1)^4} J(R, -1/2) - \frac{(3 + x_t)}{6(x_t - 1)^4} J(R, 5/2) \\
&- \frac{1}{6(x_t - 1)^4} \left[x_t(1 + 3x_t) - (-2 + 3x_t)(1 + (-10 + x_t)x_t) \right] J(R, 1/2) \\
&\left. + \frac{1}{6(x_t - 1)^4} \left[(-2 + 3x_t)(3 + x_t) - (1 + (-10 + x_t)x_t) \right] J(R, 3/2) \right] \tag{2.24}
\end{aligned}$$

and

$$\begin{aligned}
\sum_{n=1}^{\infty} E'_n(x_t, x_n) = & -\frac{x_t(-17 + (-8 + x_t)x_t)}{24(x_t - 1)^3} \\
& + \frac{\pi M_W R}{4} \left[\int_0^1 dy (y^{1/2} + 2y^{3/2} - 3y^{5/2}) \coth(\pi M_W R \sqrt{y}) \right. \\
& - \frac{x_t(1 + 3x_t)}{(x_t - 1)^4} J(R, -1/2) + \frac{(3 + x_t)}{(x_t - 1)^4} J(R, 5/2) \\
& + \frac{1}{(x_t - 1)^4} \left[x_t(1 + 3x_t) - (1 + (-10 + x_t)x_t) \right] J(R, 1/2) \\
& \left. - \frac{1}{(x_t - 1)^4} [(3 + x_t) - (1 + (-10 + x_t)x_t)] J(R, 3/2) \right] \quad (2.25)
\end{aligned}$$

where

$$J(R, \alpha) = \int_0^1 dy y^\alpha [\coth(\pi M_W R \sqrt{y}) - x_t^{1+\alpha} \coth(\pi m_t R \sqrt{y})]. \quad (2.26)$$

The Wilson coefficient C_9 given by Eq. (2.5) in the naive dimensional regularization (NDR) scheme can be generalized in the ACD model as

$$C_9(\mu, 1/R) = P_0^{NDR} + \frac{Y(x_t, 1/R)}{\sin^2 \theta_W} - 4Z(x_t, 1/R) + P_E E(x_t, 1/R) \quad (2.27)$$

where $P_0^{NDR} = 2.6 \pm 0.25$ and P_E is numerically negligible. The functions $Y(x_t, 1/R)$ and $Z(x_t, 1/R)$ are defined as

$$\begin{aligned}
Y(x_t, 1/R) &= Y_0(x_t) + \sum_{n=1}^{\infty} C_n(x_t, x_n), \\
Z(x_t, 1/R) &= Z_0(x_t) + \sum_{n=1}^{\infty} C_n(x_t, x_n), \quad (2.28)
\end{aligned}$$

with the functions $Y_0(x_t)$ and $Z_0(x_t)$ given in Eq. (2.6),

$$C_n(x_t, x_n) = \frac{x_t}{8(x_t - 1)^2} \left[x_t^2 - 8x_t + 7 + (3 + 3x_t + 7x_n - x_t x_n) \ln \frac{x_t + x_n}{1 + x_n} \right], \quad (2.29)$$

and

$$\begin{aligned} \sum_{n=1}^{\infty} C_n(x_t, x_n) &= \frac{x_t(7 - x_t)}{16(x_t - 1)} - \frac{\pi M_W R x_t}{16(x_t - 1)^2} \\ &\times \left[3(1 + x_t)J(R, -1/2) + (x_t - 7)J(R, 1/2) \right]. \end{aligned} \quad (2.30)$$

Finally, the scale independent C_{10} is given by

$$C_{10} = -\frac{Y(x_t, 1/R)}{\sin^2 \theta_W} \quad (2.31)$$

where $Y(x_t, 1/R)$ is defined in Eq. (2.28).

CHAPTER 3

ANALYSIS OF $B_c \rightarrow (D_s, D)\ell^+\ell^-$ DECAYS IN THE ACD MODEL

It is well known that the rare B_c meson decays, as being FCNC processes, are sensitive to the structure of the SM, and its possible extensions. Therefore, these decays may provide an essential tool to investigate the new physics prior to extension of it.

Considering the new physics beyond the SM, extra dimensions have special place. Extra dimensions with UED are quite special because of the propagation of all the SM particles in extra dimensions. The compactification of the UED allows KK partners of the SM fields in the four-dimensional theory and also KK modes without corresponding the SM partners. Among the UED, the ACD model is a simpler scenario, i.e. it includes only a single UED which is the compactification radius, and through the infinite KK modes the SM particles are available in the zero mode.

In rare B meson decays, the effects of the new physics appears in two different ways, one of which is the new contributions to the Wilson coefficients available in the SM, and the other is through the new operators in the effective Hamiltonian that are absent in the SM. In the ACD model, there are not any new operators, i.e. no new Wilson coefficients, contribute to the effective Hamiltonian. We will use Wilson coefficients already exist in the SM but they need to be modified according to the ACD model which have been done in [35, 36] at NLL order and given in Section 2.3.

The inverse of the of the compactification radius, $1/R$, is the only new parameter which needs to be a bound put on. For this purpose, in many experimental and theoretical works this parameter have been discussed. Tevatron experiments put the bound $1/R \geq 300 \text{ GeV}$. Analysis of the anomalous magnetic moment and $B \rightarrow X_s \gamma$ [38] also lead to the bound $1/R \geq 300 \text{ GeV}$. In the study of $B \rightarrow K^* \gamma$ decay [37], the results restrict

R to be $1/R \geq 250 \text{ GeV}$. Also, in [39] this bound is given as $1/R \geq 330 \text{ GeV}$. In a few recent works, the theoretical study of $B \rightarrow K\eta\gamma$ matches with experimental data if $1/R \geq 250 \text{ GeV}$ [40], using the experimental result and theoretical prediction on the branching ratio of $\Lambda_b \rightarrow \Lambda\mu^+\mu^-$, the lower bound was obtained to be approximately $1/R \sim 250 \text{ GeV}$ [41] and also theoretical study of branching ratio in $B_c \rightarrow D_s^*\ell^+\ell^-$ decay estimate $\sim 250 \text{ GeV}$ for $1/R$ [42]. So, the lower bound on $1/R$ seems to be $\sim 250 \text{ GeV}$ or $\sim 350 \text{ GeV}$. In this thesis, we will consider $1/R$, in the electroweak scale from 200 GeV up to 1000 GeV , however, under the points discussed above $1/R = 250 - 350 \text{ GeV}$ region will be taken more common bound region and more attention will pay to.

The effective Hamiltonian of several FCNC processes [35, 36], semileptonic and radiative decays of B mesons [43–52] and FCNC baryonic decays [41, 53, 54] have been investigated in the ACD model.

We analyze the physical observables in terms of the compactification factor and the form factors since $B_c \rightarrow D_{q'}\ell^+\ell^-$ is an exclusive decay. The form factors are the matrix elements of the effective Hamiltonian between the initial and final mesons states. These hadronic transition matrix elements are related to the nonperturbative sector of the QCD and should be calculated by means of a nonperturbative approach. Thus, their theoretical calculation yield the main uncertainty in the prediction of the exclusive rare decays. The form factors for $B_c \rightarrow D_{q'}\ell^+\ell^-$ process have been calculated using different quark models [21–25] and three-point QCD sum rules [26]. In this thesis, we will use the form factors calculated in the constitute quark model [21].

Various kinematical analysis of the $B_c \rightarrow D_{q'}\ell^+\ell^-$ decays have been studied in the works mentioned above and also the new physics effects have been investigated in a model independent analysis [55].

In this chapter, we will first introduce the quark level effective Hamiltonian and the Wilson coefficients in the ACD Model in accordance with the previous chapter. Additionally, compare the modified Wilson coefficients with the SM ones. Using the

hadronic form factors, we will get the transition matrix element and then the dilepton mass spectrum. Finally, discuss the numerical results for the differential and total branching ratios by using the numerical values of the form factors.

3.1. EFFECTIVE HAMILTONIAN AND WILSON COEFFICIENTS

The $B_c \rightarrow D_{q'} \ell^+ \ell^-$ decays are described at the quark level by $b \rightarrow s, d \ell^+ \ell^-$ transition in the effective Hamiltonian approach in the SM and can be written as follows [15]:

$$\begin{aligned} \mathcal{H}_{eff} = & \frac{G_F \alpha}{\sqrt{2}\pi} V_{tb} V_{tq'}^* \left[C_9^{eff} (\bar{q}' \gamma_\mu L b) \bar{\ell} \gamma^\mu \ell + C_{10} (\bar{q}' \gamma_\mu L b) \bar{\ell} \gamma^\mu \gamma_5 \ell \right. \\ & \left. - 2C_7^{eff} m_b (\bar{q}' i \sigma_{\mu\nu} \frac{q^\nu}{q^2} R b) \bar{\ell} \gamma^\mu \ell \right] \end{aligned} \quad (3.1)$$

where $q = p_{B_c} - p_{D_{q'}}$ is the momentum transfer, $q' = s, d$ and $L, R = (1 \pm \gamma_5)/2$ and C_i s are the Wilson coefficients evaluated at the b quark mass scale.

The new physics contributions in the ACD model appear by using the modified Wilson coefficients available in the SM. This can be done in terms of some periodic functions, which are function of compactification factor, $1/R$ and generalize the $F_0(x_t)$ SM functions according to

$$F(x_t, 1/R) = F_0(x_t) + \sum_{n=1}^{\infty} F_n(x_t, x_n), \quad (3.2)$$

the details of which were given in Section 2.3. Therefore, the Wilson coefficients appear in the effective Hamiltonian in Eq. (3.1) can be written as

$$\begin{aligned}
C_9^{eff}(s', 1/R) &= C_9(\mu, 1/R) \left(1 + \frac{\alpha_s(\mu)}{\pi} w(s') \right) + Y(\mu) + C_9^{res}(\mu) \\
C_7^{eff}(\mu_b, 1/R) &= \eta^{16/23} C_7(\mu_W, 1/R) \\
&\quad + \frac{8}{3} (\eta^{14/23} - \eta^{16/23}) C_8(\mu_W, 1/R) + C_2(\mu_W, 1/R) \sum_{i=1}^8 h_i \eta^{a_i} \\
C_{10} &= -\frac{Y(x_t, 1/R)}{\sin^2 \theta_W}. \tag{3.3}
\end{aligned}$$

The Wilson coefficients differ considerably from the SM values for small R . The variation of modified Wilson coefficients with respect to $1/R$ at $q^2 = 14 \text{ GeV}^2$, in which the normalization scale is fixed to $\mu = \mu_b \simeq 4.8 \text{ GeV}$, is given in Fig. 3.1. The suppression of $|C_7^{eff}|$ for $1/R = 250 - 350 \text{ GeV}$ amount to 75% – 86% relative to the SM value. $|C_{10}|$ is enhanced by 23% – 13%. The impact of the ACD on $|C_9^{eff}|$ is very small. For $1/R \gtrsim 600 \text{ GeV}$ the difference is less than 5%.

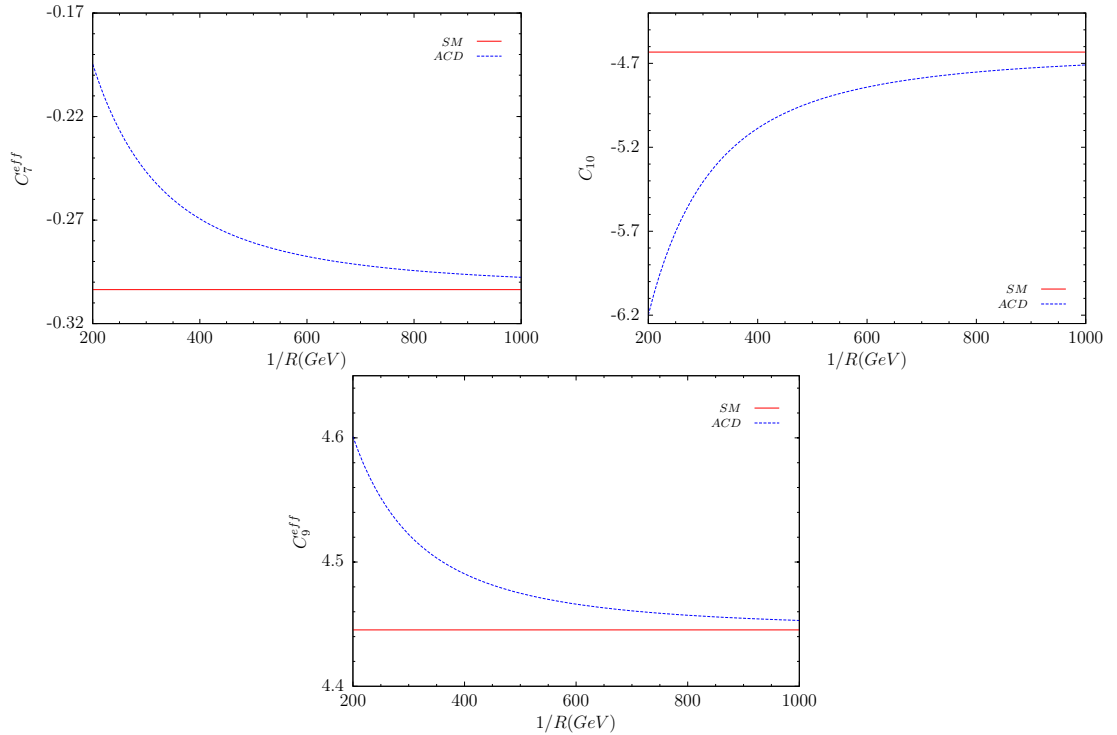


Figure 3.1. The variation of the Wilson coefficients with respect to $1/R$ at $q^2 = 14 \text{ GeV}^2$ for the normalization scale $\mu = 4.8 \text{ GeV}$.

3.2. MATRIX ELEMENTS AND DECAY RATE

The hadronic matrix elements in the exclusive $B_c \rightarrow D_{q'}\ell^+\ell^-$ decay can be obtained by sandwiching the quark level operators in the effective Hamiltonian between the initial and the final state mesons. The parts of transition currents containing γ_5 do not contribute, so the non-vanishing matrix elements are parameterized in term of form factors as follows [56]

$$\begin{aligned} \langle D(P_{D_{q'}}) | \bar{q}' i \sigma_{\mu\nu} q^\nu (1 + \gamma_5) b | B(P_{B_c}) \rangle &= -\frac{f_T}{m_{B_c} + m_{D_{q'}}} \\ &\times \left[(P_{D_{q'}} + P_{B_c})_\mu q^2 - q_\mu (m_{B_c}^2 - m_{D_{q'}}^2) \right] \\ \langle D(P_{D_{q'}}) | \bar{q}' \gamma_\mu (1 - \gamma_5) b | B(P_{B_c}) \rangle &= f_+(P_{B_c} + P_{D_{q'}})_\mu + f_- q_\mu. \end{aligned} \quad (3.4)$$

The transition amplitude of the $B_c \rightarrow D_{q'}\ell^+\ell^-$ decay can be written using the effective Hamiltonian and Eq. (3.4) as

$$\begin{aligned} \mathcal{M}(B_c \rightarrow D_{q'}\ell^+\ell^-) &= \frac{G_F \alpha}{2\sqrt{2}\pi} V_{tb} V_{tq'}^* \\ &\times \left\{ \bar{\ell} \gamma^\mu \ell [A(P_{B_c} + P_{D_{q'}})_\mu + B q_\mu] + \bar{\ell} \gamma^\mu \gamma_5 \ell [C(P_{B_c} + P_{D_{q'}})_\mu + D q_\mu] \right\} \end{aligned} \quad (3.5)$$

with

$$\begin{aligned} A &= C_9 f_+ + 2C_7 m_b \frac{f_T}{m_B + m_D} \\ B &= C_9 f_- - (m_B^2 - m_D^2) \frac{f_T}{m_B + m_D} \\ C &= C_{10} f_+ \\ D &= C_{10} f_- . \end{aligned} \quad (3.6)$$

The next task is the calculation of the decay rate of $B_c \rightarrow D_{q'}\ell^+\ell^-$, which is determined from the following expression:

$$\Gamma = \frac{(2\pi)^4}{2E_{B_c}} \int \frac{d^3\vec{p}_1}{(2\pi)^3 2E_1} \frac{d^3\vec{p}_2}{(2\pi)^3 2E_2} \frac{d^3\vec{p}_{D_{q'}}}{(2\pi)^3 2E_{D_{q'}}} |\mathcal{M}|^2 \delta^4(q - p_1 - p_2), \quad (3.7)$$

where \mathcal{M} is the transition amplitude of the decay. When the final state polarizations are not measured, we must sum over their spin states using the following projection operators

$$\begin{aligned}\sum_{spin} \ell(p_1)\bar{\ell}(p_1) &= \not{p}_1 - m_\ell, \\ \sum_{spin} \ell(p_2)\bar{\ell}(p_2) &= \not{p}_2 + m_\ell.\end{aligned}\tag{3.8}$$

In the center of mass (CM) frame of the dileptons $\ell^+\ell^-$, where we take $z = \cos\theta$ and θ is the angle between the momentum of the B_c -meson and that of ℓ^- , double differential decay rate is found to be

$$\frac{d\Gamma}{dsdz} = \frac{1}{2^9\pi^3} m_B \sqrt{\lambda} v |\mathcal{M}|^2\tag{3.9}$$

where $s = q^2/m_{B_c}^2$, $\lambda = 1 + r^2 + s^2 - 2r - 2s - 2rs$, $r = m_{D_{q'}}^2/m_{B_c}^2$, $v = \sqrt{1 - 4m_\ell^2/sm_{B_c}^2}$ and

$$\begin{aligned}|\mathcal{M}|^2 &= \left| \frac{G_F\alpha}{2\sqrt{2}\pi} V_{tb}V_{tq'}^* \right|^2 \left[4m_{B_c}^2 \lambda (1 - v^2 z^2) (|A|^2 + |C|^2) + 16m_{B_c}^2 m_\ell^2 (2r + 2 - s) |C|^2 \right. \\ &\quad \left. + 16m_{B_c}^2 m_\ell^2 s |D|^2 + 16m_{B_c}^2 m_\ell^2 (r - 1) \text{Re}[CD^*] \right].\end{aligned}\tag{3.10}$$

Integrating over the angular dependence of the double differential decay rate, following dilepton mass spectrum is obtained

$$\frac{d\Gamma}{ds} = \frac{G^2\alpha^2 m_B}{2^{12}\pi^5} |V_{tb}V_{ts}^*|^2 \sqrt{\lambda} v \Delta\tag{3.11}$$

where

$$\begin{aligned} \Delta_{D_{q'}} &= \frac{4}{3}m_{B_c}^4(3-v^2)\lambda(|A|^2+|C|^2)+4m_{B_c}^4s(2+r-s)(1-v^2)|C|^2 \\ &+16m_{B_c}^2m_\ell^2s|D|^2+32m_{B_c}^2m_\ell^2(1-r)Re(CD^*). \end{aligned} \quad (3.12)$$

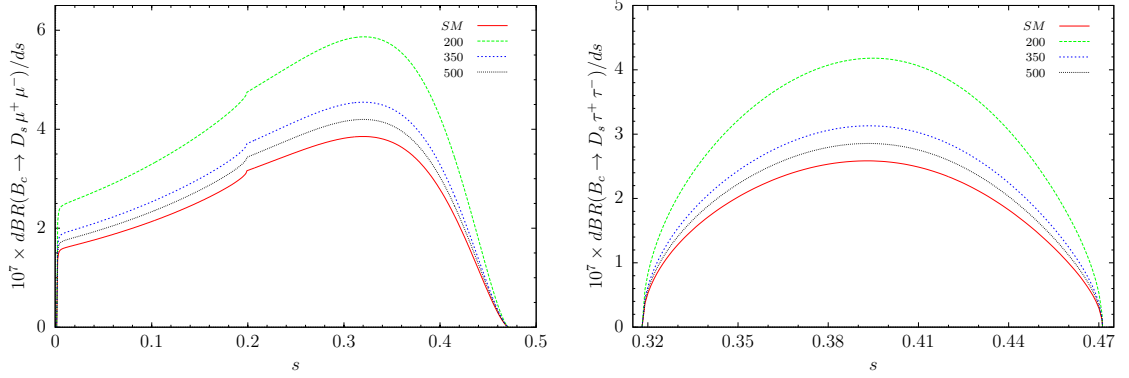


Figure 3.2. The dependence of differential branching ratio on s without resonance contributions for $B_c \rightarrow D_s \ell^+ \ell^-$. (In the legend $1/R = 200, 350, 500$ GeV.)

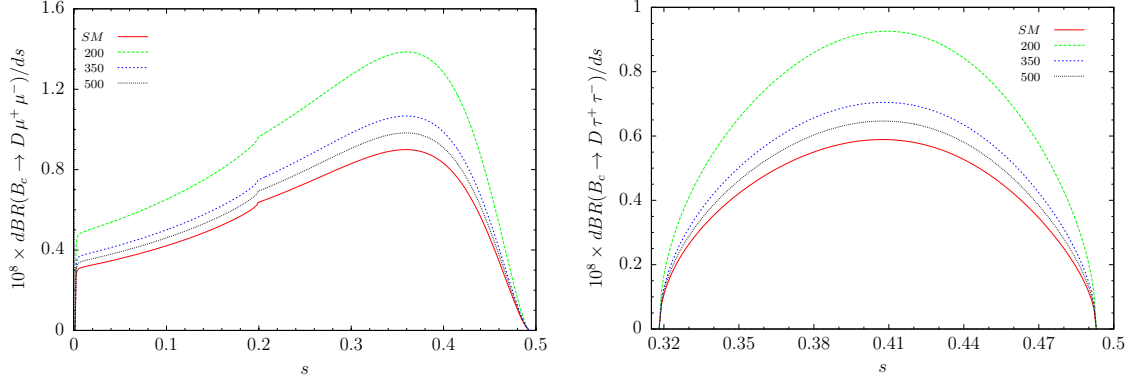


Figure 3.3. The dependence of differential branching ratio on s without resonance contributions for $B_c \rightarrow D \ell^+ \ell^-$.

In the numerical analysis of physical observables, we have used the input parameters given in Appndix A and the values that are not given are taken from [30]. In addition, to make numerical predictions, we also need the explicit forms of the form factors f_+ , f_- and f_T . In our numerical analysis we used the results of [21], calculated in the

constitute quark model and q^2 parametrization is given by

$$F(q^2) = \frac{F(0)}{1 - a(q^2/m_{B_c}^2) + b(q^2/m_{B_c}^2)^2}, \quad (3.13)$$

where the values of parameters $F(0)$, a and b for the $B_c \rightarrow (D_s, D)$ decays are listed in Table 3.1. To obtain the branching ratio, we integrate Eq. (3.11) in the

Table 3.1. $B_c \rightarrow D_{s,d}$ form factors calculated in the constitute quark model.

$B_c \rightarrow D_s \ell^+ \ell^-$	$F(0)$	a	b
f_+	0.165	- 3.40	3.21
f_-	-0.186	- 3.51	3.38
f_T	-0.258	- 3.41	3.30
$B_c \rightarrow D \ell^+ \ell^-$	$F(0)$	a	b
f_+	0.126	- 3.35	3.03
f_-	-0.141	- 3.63	3.55
f_T	-0.199	- 3.52	3.38

allowed physical region. While taking the long-distance contributions into account we introduce some cuts around J/ψ and $\psi(2s)$ resonances to minimize the hadronic uncertainties. The integration region for q^2 is divided into three parts for μ as $4m_\mu^2 \leq q^2 \leq (m_{J/\psi} - 0.02)^2$, $(m_{J/\psi} + 0.02)^2 \leq q^2 \leq (m_{\psi(2s)} - 0.02)^2$ and $(m_{\psi(2s)} + 0.02)^2 \leq q^2 \leq (m_{B_c} - m_{D_s^*})^2$. In the case of, τ we have $4m_\tau^2 \leq q^2 \leq (m_{\psi(2s)} - 0.02)^2$ and $(m_{\psi(2s)} + 0.02)^2 \leq q^2 \leq (m_{B_c} - m_{D_s^*})^2$, the same as in [42].

The differential branching ratios are calculated with and without resonance contributions and s dependence for $1/R = 200, 350, 500 \text{ GeV}$ are presented in Figs. 3.2- 3.5 for $B_c \rightarrow (D_s, D)\ell^+\ell^-$. One can notice, the change in differential decay rate and difference between the SM results and new effects in the figures. The maximum deviation is around $s = 0.32$ (0.39) in Fig. 3.2 and $s = 0.36$ (0.40) in Fig. 3.3 for μ (τ). At these s values, the deviation is $\sim 50\%$ more than that of the SM

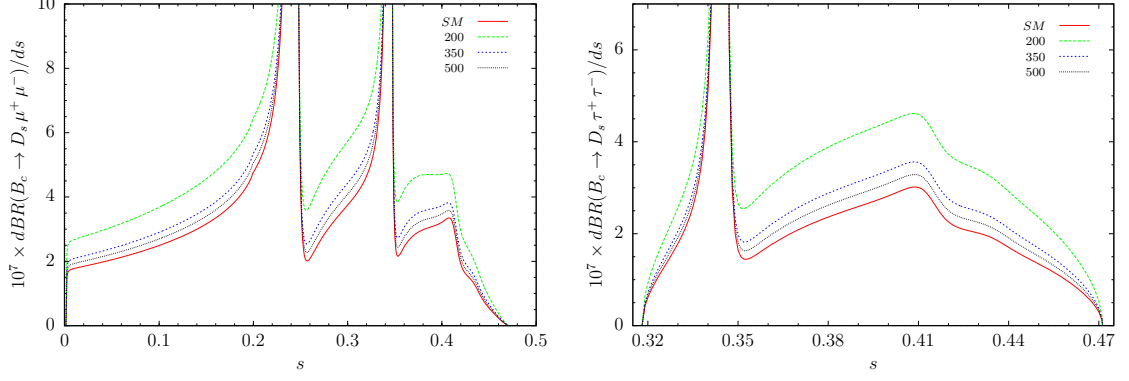


Figure 3.4. The dependence of differential branching ratio on s with resonance contributions for $B_c \rightarrow D_s l^+ l^-$.

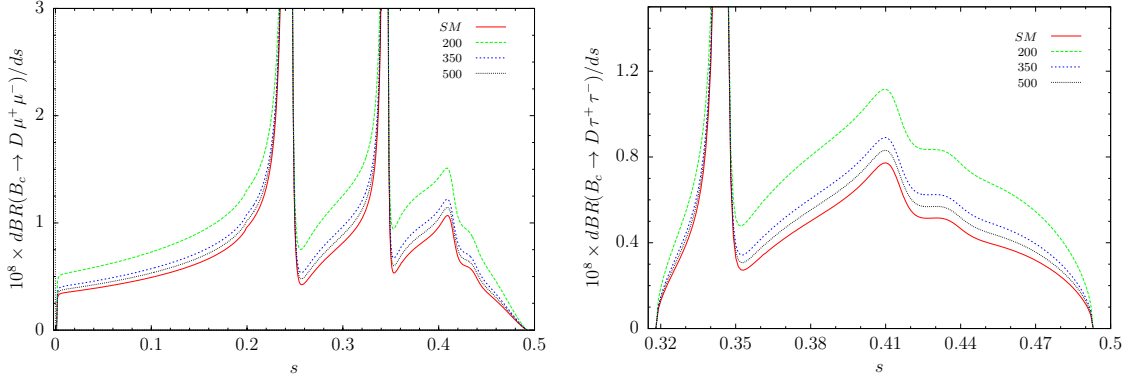


Figure 3.5. The dependence of differential branching ratio on s without resonance contributions for $B_c \rightarrow D l^+ l^-$.

results for $1/R = 200 \text{ GeV}$ in all decay channels and $\sim 20\%$ for $1/R = 350 \text{ GeV}$. For $1/R \gtrsim 500 \text{ GeV}$, the deviation becomes $\sim 10\%$ and less. Considering the resonance effects, the differential decay rates also differ from their SM values as $1/R \rightarrow 200 \text{ GeV}$, which can be seen in Figs. 3.4 and 3.5. So, studying differential decay rate, particularly in $1/R = 200 - 350 \text{ GeV}$ region, can be an appropriate tool for searching the effect of extra dimension.

To introduce the contributions of the ACD model on the branching ratio, we present $1/R$ dependent ratios with and without resonance cases in Figs. 3.6 and 3.7. The common feature is that as $1/R$ increases, the branching ratios approach to their SM values. In all decay channels, for $1/R \simeq 500 \text{ GeV}$ the deviations are more than 10% from their SM values. Additionally, around $1/R \simeq 200 \text{ GeV}$ the ACD contribution is

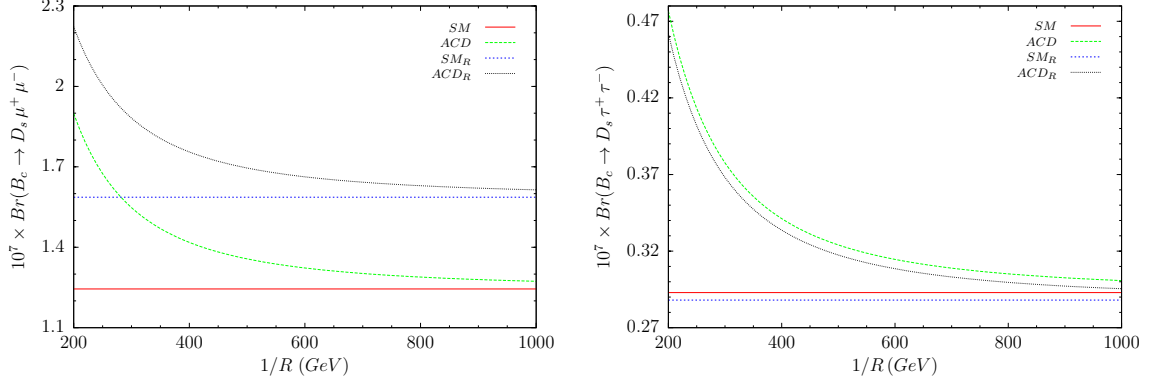


Figure 3.6. The dependence of branching ratio on $1/R$ with and without resonance contributions for $B_c \rightarrow D_s \ell^+ \ell^-$.

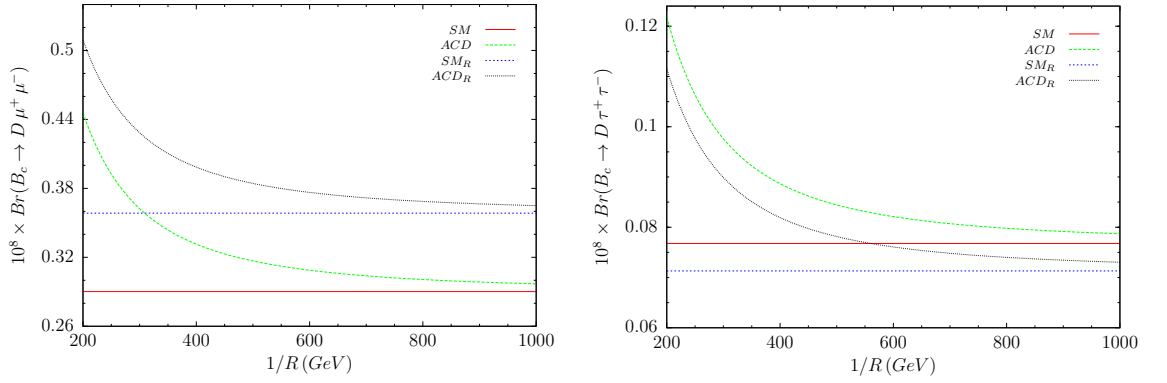


Figure 3.7. The dependence of branching ratio on $1/R$ with and without resonance contributions for $B_c \rightarrow D \ell^+ \ell^-$.

more than 50%. Keeping the discussion on lower bound on $1/R$ in mind once again, in the region $1/R \simeq 350 - 250 \text{ GeV}$ the branching ratios increase with an average of (25 – 35)%. So, the calculated branching ratios without resonance contributions for the SM and in between these bounds we find,

$$Br(B_c \rightarrow D_s \mu^+ \mu^-) = (1.24, 1.47 - 1.67) \times 10^{-7}$$

$$Br(B_c \rightarrow D_s \tau^+ \tau^-) = (0.29, 0.36 - 0.41) \times 10^{-7}$$

$$Br(B_c \rightarrow D \mu^+ \mu^-) = (0.29, 0.34 - 0.39) \times 10^{-8}$$

$$Br(B_c \rightarrow D \tau^+ \tau^-) = (0.077, 0.092 - 0.106) \times 10^{-8}.$$

Here, the first value in any branching ratios above is corresponding to the SM, while

the rests are for $1/R = 350 - 250 \text{ GeV}$. A similar behavior is valid for resonance case which can be followed by the figures.

Adding the uncertainty on the form factors may influence the contribution range of the ACD model. However, the variation of the branching ratio, calculated with the central values of form factors, in the ACD model for different $1/R$ s with the SM values, can be considered as a signal of new physics and an evidence of existence of extra dimension.

CHAPTER 4

LEPTON POLARIZATIONS IN $B_c \rightarrow (D_s, D)\ell^+\ell^-$ DECAYS

The polarization asymmetries of the final state leptons can be very useful for testing the SM results, and also a powerful tool for searching new physics contributions. The final state leptons in the decays can have longitudinal, transverse and normal polarizations. The transverse polarization is the component lying in the decay plane and normal is the one that is normal to the decay plane.

In the $B_s \rightarrow D_{s,d}\ell^+\ell^-$ decays, we will search the polarization asymmetries for further investigation of the SM and discuss the possible effects of the ACD model, for μ and τ as final state leptons. While doing this, we analyze possible polarization effects in resonance and non-resonance cases. Also, we introduce the variation of polarizations with respect to transferred momentum and $1/R$ dependence of averaged polarizations.

In this chapter, after introducing the definition of polarizations, starting with the effective Hamiltonian, we calculate the analytical expressions of various lepton polarization asymmetries, introduce the obtained results with a couple of figures and give a complete analysis and discussion.

4.1. LEPTON POLARIZATION ASYMMETRY

We first introduce the spin projection operators given by

$$\begin{aligned} P^- &= \frac{1}{2}(1 + \gamma_5 \not{\not{p}}_j^-) \\ P^+ &= \frac{1}{2}(1 - \gamma_5 \not{\not{p}}_j^-) \end{aligned} \tag{4.1}$$

for ℓ^- and ℓ^+ , respectively. Here, $j = L, T, N$ denotes the longitudinal, transverse and normal components of the polarizations, respectively. The four vectors S_μ^\pm , which satisfy

$$S^- \cdot p_1 = S^+ \cdot p_2 = 0 \quad \text{and} \quad S^- \cdot S^- = S^+ \cdot S^+ = -1, \quad (4.2)$$

are defined in the rest frame of ℓ^- and ℓ^+ . Using the convention followed by previous works [57, 58], in the rest frame of ℓ^- we define the orthogonal unit vectors S_i^- , for the polarization of the leptons along the longitudinal, transverse and normal directions as

$$\begin{aligned} S_L^- &\equiv (0, \vec{e}_L) = \left(0, \frac{\vec{p}_\ell}{|\vec{p}_\ell|}\right), \\ S_T^- &\equiv (0, \vec{e}_T) = (0, \vec{e}_N \times \vec{e}_L), \\ S_N^- &\equiv (0, \vec{e}_N) = \left(0, \frac{\vec{p}_{D_{q'}} \times \vec{p}_\ell}{|\vec{p}_{D_{q'}} \times \vec{p}_\ell|}\right), \end{aligned} \quad (4.3)$$

where \vec{p}_ℓ and $\vec{p}_{D_{q'}}$ are the three momenta of ℓ^- and $D_{q'}$ meson in the CM frame of final state leptons, respectively. The longitudinal unit vector S_L^- is boosted by Lorentz transformation,

$$S_{L,CM}^- = \left(\frac{|\vec{p}_\ell|}{m_\ell}, \frac{E_\ell \vec{p}_\ell}{m_\ell |\vec{p}_\ell|}\right), \quad (4.4)$$

while vectors of perpendicular directions remain unchanged under the Lorentz boost. The differential decay rate of $B_c \rightarrow D_{q'} \ell^+ \ell^-$ for any spin direction \vec{n}^- of the ℓ^- can be written in the following form

$$\frac{d\Gamma(\vec{n}^-)}{ds} = \frac{1}{2} \left(\frac{d\Gamma}{ds}\right)_0 \left[1 + \left(P_L \vec{e}_L^- + P_N \vec{e}_N^- + P_T \vec{e}_T^-\right) \cdot \vec{n}^-\right], \quad (4.5)$$

where $(d\Gamma/ds)_0$ corresponds to the unpolarized decay rate, the explicit form of which is given in Eqn. (3.11).

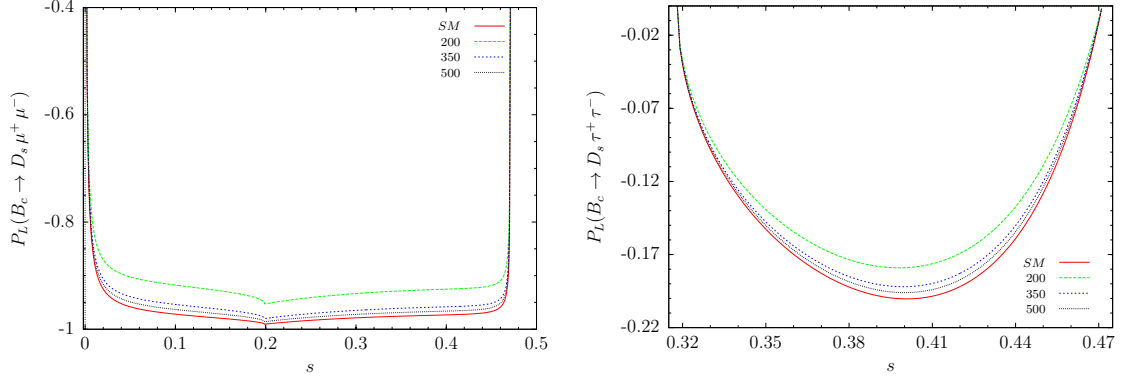


Figure 4.1. The dependence of longitudinal polarization on s without resonance contributions for $B_c \rightarrow D_s \ell^+ \ell^-$.

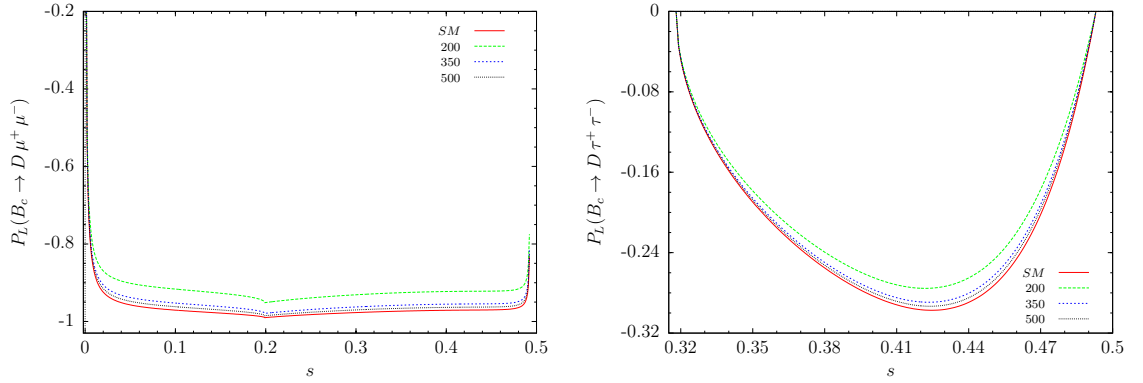


Figure 4.2. The dependence of longitudinal polarization on s without resonance contributions for $B_c \rightarrow D \ell^+ \ell^-$.

The polarizations P_L^- , P_T^- and P_N^- in Eq. (4.5) are defined by the equation

$$P_i^-(s) = \frac{\frac{d\Gamma}{ds}(\mathbf{n}^- = \mathbf{e}_i^-) - \frac{d\Gamma}{ds}(\mathbf{n}^- = -\mathbf{e}_i^-)}{\frac{d\Gamma}{ds}(\mathbf{n}^- = \mathbf{e}_i^-) + \frac{d\Gamma}{ds}(\mathbf{n}^- = -\mathbf{e}_i^-)}.$$

Here, P_L^- and P_T^- represent the longitudinal and transversal asymmetries, respectively, of the charged lepton ℓ^- in the decay plane, and P_N^- is the normal component to both of them. Calculations yield the explicit form of the longitudinal polarization for $B_c \rightarrow D_{s,d} \ell^+ \ell^-$ as

$$P_L^- = \frac{8m_{B_c}^2 v}{\Delta} \left[\frac{2}{3} m_{B_c}^2 \lambda \text{Re}(AC^*) \right] \quad (4.6)$$

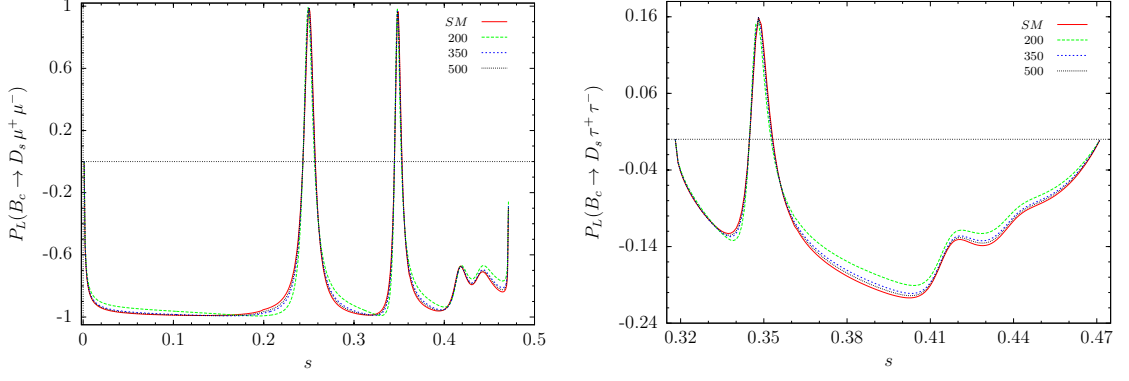


Figure 4.3. The dependence of longitudinal polarization on s with resonance contributions for $B_c \rightarrow D_s \ell^+ \ell^-$.

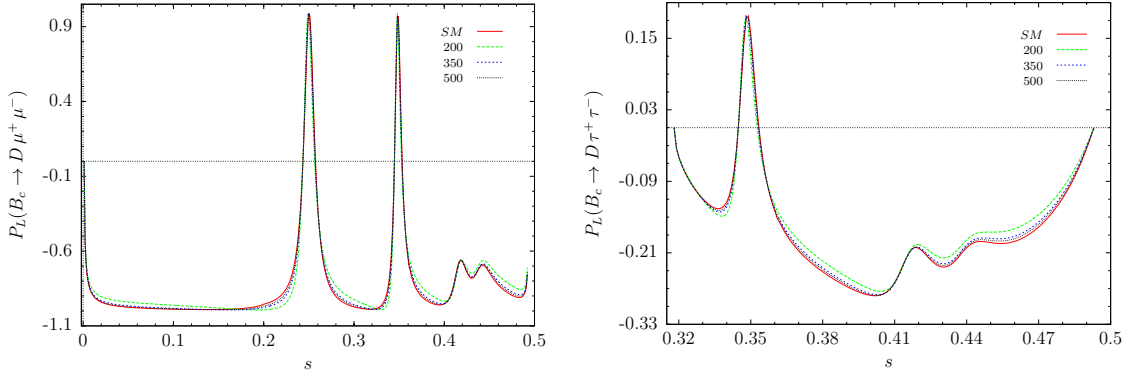


Figure 4.4. The dependence of longitudinal polarization on s with resonance contributions for $B_c \rightarrow D \ell^+ \ell^-$.

and similarly, the transverse polarization is given by

$$P_T^- = \frac{4m_{B_c}^3 m_\ell \pi \sqrt{s\lambda}}{\Delta} \left[\frac{(r-1)}{s} \text{Re}[AC^*] + \text{Re}[AD^*] \right]. \quad (4.7)$$

The normal component of polarization is zero so we have not stated its explicit form.

We eliminate the dependence of the lepton polarizations on s in order to clarify dependence on $1/R$, by considering the averaged forms over the allowed kinematical

region. The averaged lepton polarizations are defined by

$$\langle P_i \rangle = \frac{\int_{(2m_\ell/m_{B_c})^2}^{(1-m_{D_s^*}/m_{B_c})^2} P_i \frac{d\mathcal{B}}{ds} ds}{\int_{(2m_\ell/m_{B_c})^2}^{(1-m_{D_s^*}/m_{B_c})^2} \frac{d\mathcal{B}}{ds} ds}. \quad (4.8)$$

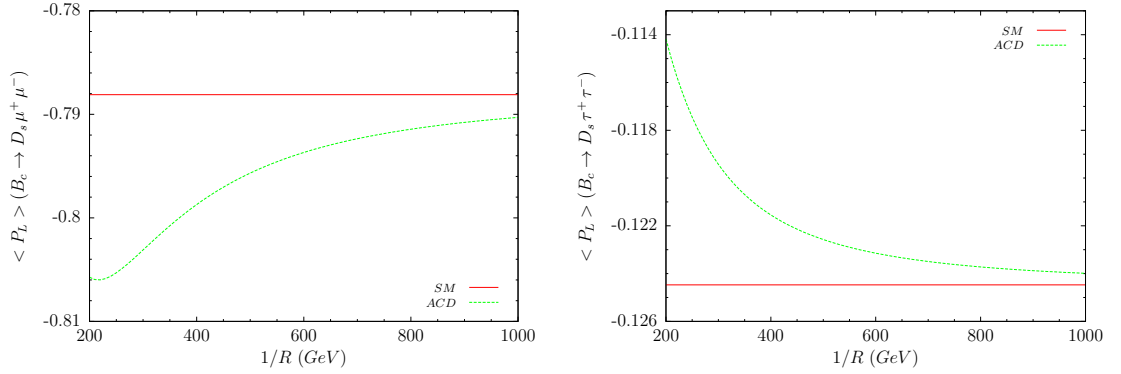


Figure 4.5. The dependence of longitudinal polarization on $1/R$ with resonance contributions for $B_c \rightarrow D\ell^+\ell^-$.

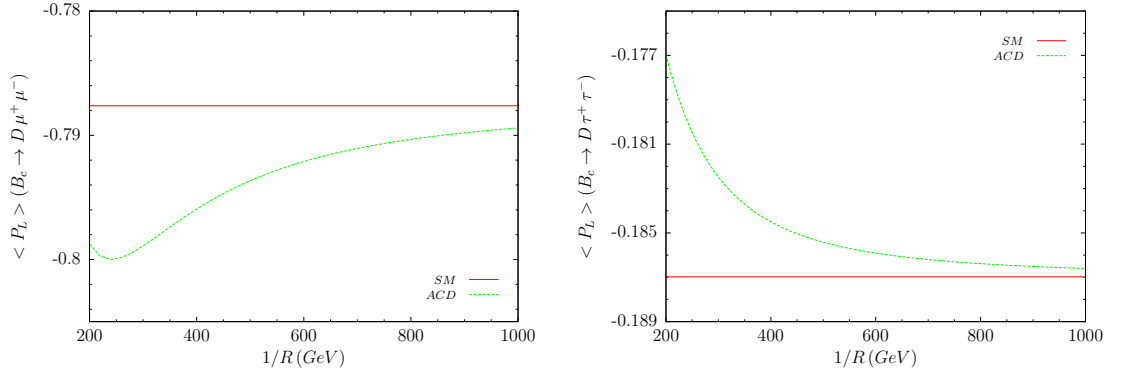


Figure 4.6. The dependence of longitudinal polarization on $1/R$ with resonance contributions for $B_c \rightarrow D\ell^+\ell^-$.

4.2. ANALYSIS OF LEPTON POLARIZATION

The dependence of longitudinal polarization on s without resonance contributions are given by Figs. 4.1–4.2. As $1/R$ approaches to 200 GeV , the longitudinal polarization differ from the SM values, slightly. This is more clear in $0.34 (0.35) \lesssim s \lesssim 0.45 (0.47)$

for $B_c \rightarrow D_s(D)\tau^+\tau^-$ decay, respectively. For μ channels, the deviation is valid in all s range, excluded the minimal and maximal points of s . In $B_c \rightarrow D_s(D)\mu^+\mu^-$ decay, the difference is, for example at $s \sim 0.38$, 5% (3%), respectively, for $1/R = 200 \text{ GeV}$. For $B_c \rightarrow D_s(D)\tau^+\tau^-$ decay the results are more significant that is at $s \sim 0.40$ (0.42), the variation for $1/R = 200 \text{ GeV}$ is 12% (8%), respectively. Including resonance contributions, in addition to the above effects, deviation between the resonant and nonresonant values increases as $1/R \rightarrow 200 \text{ GeV}$, Figs. 4.3–4.4.

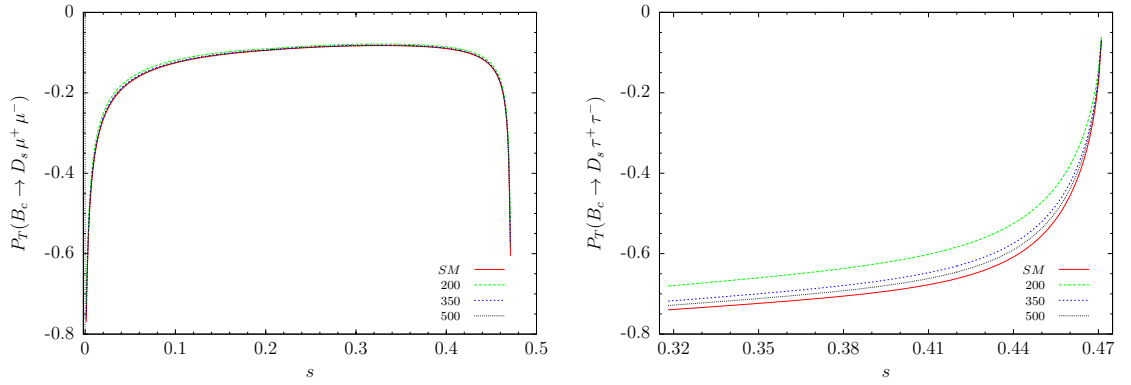


Figure 4.7. The dependence of transverse polarization on s without resonance contributions for $B_c \rightarrow D_s l^+ l^-$.

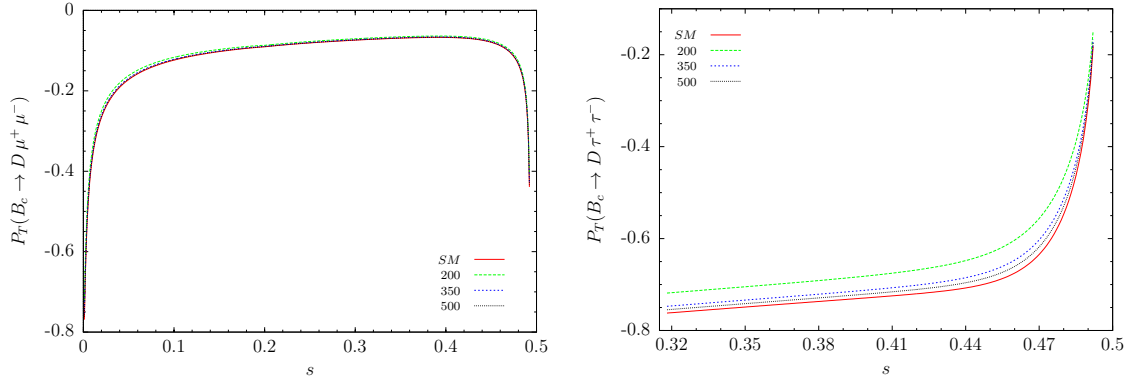


Figure 4.8. The dependence of transverse polarization on s without resonance contributions for $B_c \rightarrow D l^+ l^-$.

The $1/R$ dependant average longitudinal polarizations are given in Figs. 4.5 and 4.6. As it can be seen from the figures, the maximum deviation is 2% for μ channels and 9% (6%) for $B_c \rightarrow D_s(D)\tau^+\tau^-$, respectively, at $1/R = 200 \text{ GeV}$.

The variation of transversal polarization with respect to s are given by Figs. 4.7–4.10. In μ channels the difference is negligible whereas in τ channels up to $s \sim 0.46$ (0.48) for $B_c \rightarrow D_s(D)\ell^+\ell^-$ decays, respectively, the effects of the UED can be seen. At, for example, $s \sim 0.40$ (0.44), the SM value vary 5 – 12% (4 – 9%) for $1/R = 350 - 200 \text{ GeV}$, respectively. Finally, the average transversal polarization can be followed by Figs. 4.11 and 4.12. For the μ channels the maximum deviation is 2% and for $B_c \rightarrow D_s(D)\tau^+\tau^-$ that is 10%(6%) at $1/R = 200 \text{ GeV}$.

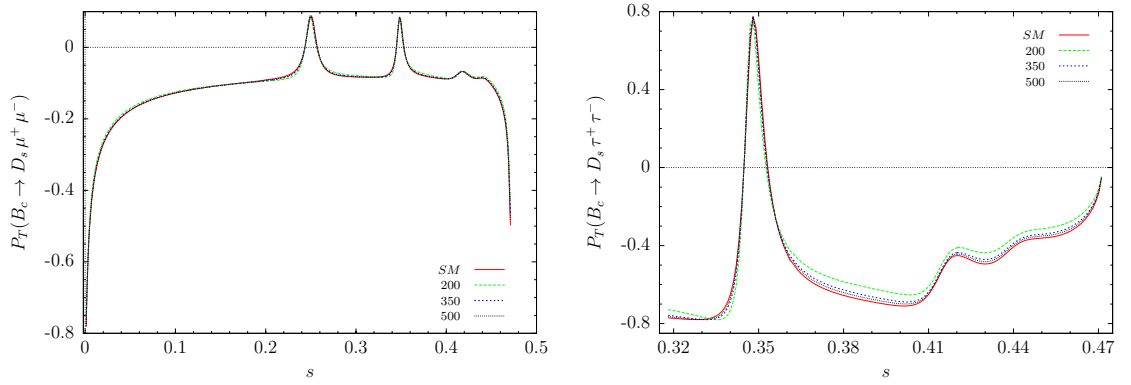


Figure 4.9. The dependence of transverse polarization on s with resonance contributions for $B_c \rightarrow D_s \ell^+ \ell^-$.

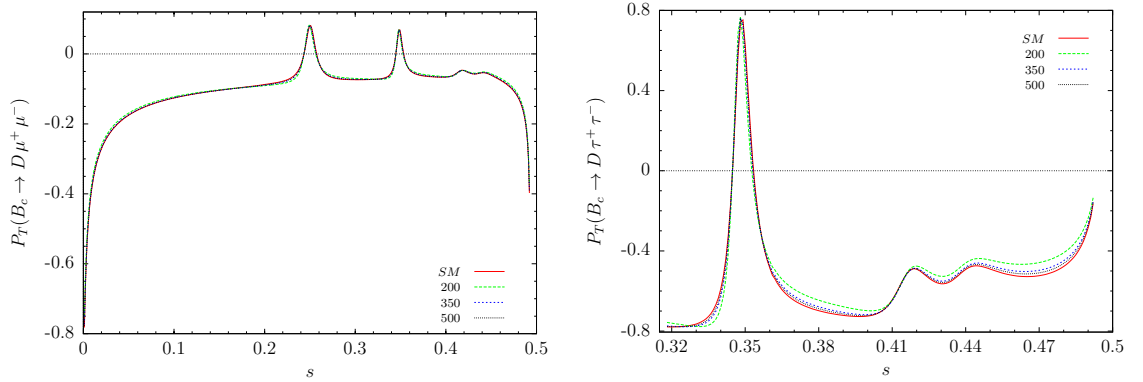


Figure 4.10. The dependence of transverse polarization on s with resonance contributions for $B_c \rightarrow D \ell^+ \ell^-$.

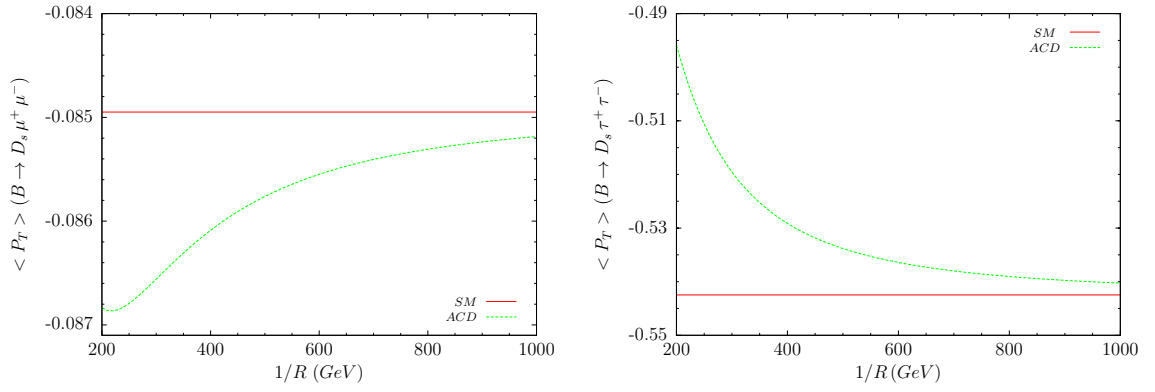


Figure 4.11. The dependence of transverse polarization on $1/R$ with resonance contributions for $B_c \rightarrow D_s \ell^+ \ell^-$.

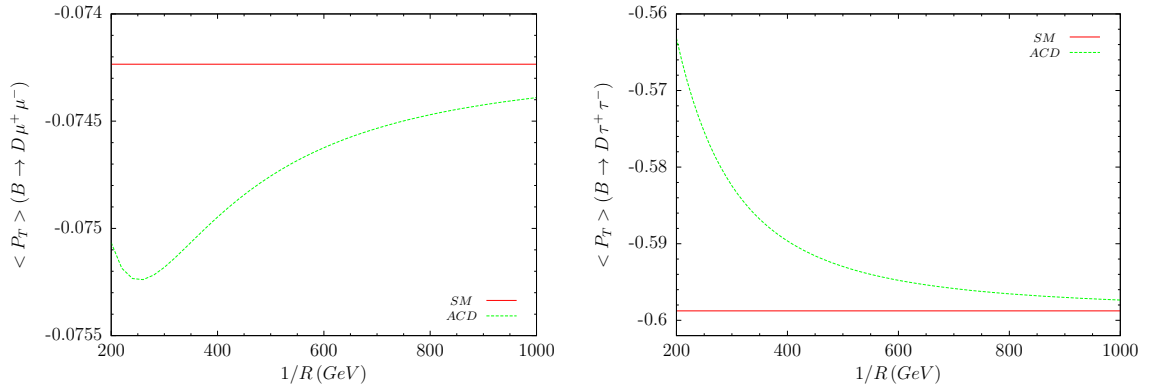


Figure 4.12. The dependence of transverse polarization on $1/R$ with resonance contributions for $B_c \rightarrow D \ell^+ \ell^-$.

CHAPTER 5

CONCLUSION

In this thesis, we have discussed the rare semileptonic $B_c \rightarrow D_{s,d} \ell^+ \ell^-$ decays induced by FCNC for μ and τ as the final state leptons in the SM and universal extra dimension with a single extra dimension, the ACD model. We used the hadronic form factors calculated in the constituent quark model and throughout the work, we reflected the resonance contributions on the calculations and demonstrate the results in possible plotting with respect to the compactification factor and transfer momentum.

As an overall result, we can conclude that as $1/R \rightarrow 200 \text{ GeV}$ the physical values differ from the SM results. Up to a few hundreds GeV above the considered bounds, $1/R \geq 250 \text{ GeV}$ or $1/R \geq 350 \text{ GeV}$, it is possible to see the effects of UED.

Taking the differential branching ratio into consideration, for small values of $1/R$ there comes out essential difference comparing with the SM results. For $1/R = 200 \text{ GeV}$ a maximum of $\sim 50\%$ deviation was obtained for both channels. In the considered lower bounds the effects are also seizable and up to $1/R = 500 \text{ GeV}$ the ACD contributions can be taken into consideration while searching new physics.

Considering the dependence of branching ratio on the compactification factor, the obtained results clearly show the evidence of new physics. A few GeV above the lower bound, the contribution of the ACD model is still convincing.

In searching new physics, calculation of polarization asymmetries of final state leptons is an essential tool. Here, the polarization properties of the leptons have been studied comprehensively and a full comparison with the SM was introduced. Our results show that, variation of the polarizations in μ channels are not significant, on the other hand

for τ channels, especially for $B_c \rightarrow D_s \ell^+ \ell^-$ decay, the results are encouraging. As a last note on polarization, the normal component of the lepton polarizations is zero in these decays both in the SM and in the ACD model.

The resonance, as a result of conversion of real $c\bar{c}$ into lepton pairs, contributions also added to the numerical calculations. In the resonance case, a similar behavior can be obtained and the numerical values of the observables mostly increased.

Under the discussion throughout this thesis, the sizable discrepancies between the ACD model and the SM predictions at lower values of the compactification scale, i.e. as $1/R$ approaches 1000 GeV the results get closer to their SM values, can be considered the indications of new physics and should be searched in the experiments. Technical facilities of the LHC make these decays accessible.

REFERENCES

1. Mann, R., "An Introduction to Particle Physics and the Standard Model", *CRC Press*, Boca Raton FL, 423-514 (2010).
2. Alam, M. S., *et. al.*, (CLEO Collaboration), "First measurement of the rate for the inclusive radiative penguin decay $b \rightarrow s\gamma$ ", *Int. Phys. Rev. Lett.*, 74 (15): 2885-2889 (1995).
3. Ali, A., "Review of heavy quark physics - theory", *Int. J. Mod. Phys. A*, 20: 5080-5094 (2005).
4. Abe, F., *et al.* (CDF Collaboration), "Observation of B_c mesons in $p\bar{p}$ collisions at $\sqrt{s} = 1.8\text{TeV}$ ", *Phys. Rev. D*, 58 (11): 112004-112083 (1998).
5. Colangelo, P. and De Fazio, F., "Using heavy quark spin symmetry in semileptonic B_c decays", *Phys. Rev. D*, 61 (3): 034012-034012 (2000).
6. Ivanov, M. A., Körner, J. G. and Santorelli, P., "Semileptonic decays of the B_c meson", *Phys. Rev. D*, 63 (7): 074010-074041 (2001).
7. Ivanov, M. A., Körner, J. G. and Santorelli, P., "Exclusive semileptonic and nonleptonic decays of the B_c meson", *Phys. Rev. D*, 73 (5): 054024-054043 (2006).
8. Sun, J., Yang, Y., Du, W. and Ma, H., "Study of $B_c \rightarrow B^{(*)}P, BV$ decays with QCD factorization", *Phys. Rev. D*, 77 (11): 114004-114065 (2008).
9. Altarelli, M. P. and Teubert, F., "B physics at LHCb", *Int. J. Mod. Phys. A*, 23 (32): 5117-5136 (2008).
10. Brambilla, N., *et al.*, (Quarkonium Working Group), "Heavy quarkonium physics", *CERN Report No: CERN-2005-005*, arXiv:hep-ph/0412158 (2005).
11. LHCb Collaboration, "Expression of interest for an LHCb upgrade", *CERN Report No: CERN/LHCC/2008-007* (2008).
12. Misiak, M., "The $b \rightarrow se^+e^-$ and $b \rightarrow s\gamma$ decays with next-to-leading logarithmic QCD corrections", *Nucl. Phys. B*, 393: 23-45 (1993); Erratum: *ibid B*, 439: 461-465 (1995).
13. Buras, A. J., Misiak, M., Münz, M. and Pokorski, S., "Theoretical uncertainties and phenomenological aspects of $B \rightarrow X_s\gamma$ Decay", *Nucl. Phys. B*, 424 (2): 374-398 (1994).

14. Buras, A. J. and Münz, M., “Effective Hamiltonian for $B \rightarrow X_s e^+ e^-$ beyond leading logarithms in the naive dimensional regularization and ’t Hooft-Veltman scheme”, *Phys. Rev. D*, 52 (1): 186-195 (1995).
15. Buchalla, G., Buras, A. J. and Lautenbacher, M., “Weak decays beyond leading logarithms”, *Rev. Mod. Phys.*, 68 (4): 1125-1244 (1996).
16. Antoniadis, I., “A Possible new dimension at a few TeV”, *Phys. Lett. B*, 246: 377-384 (1990).
17. Antoniadis, I., Arkani-Hamed, N., Dimopoulos S. and Dvali, G., “New dimensions at a millimeter to a fermi and superstrings at a TeV”, *Phys. Lett. B*, 436 (3-4): 257-263 (1998).
18. Arkani-Hamed, N., Dimopoulos S. and Dvali, G., “The hierarchy problem and new dimensions at a millimeter”, *Phys. Lett. B*, 429 (3-4): 263-272 (1998).
19. Arkani-Hamed, N., Dimopoulos S. and Dvali, G., “Phenomenology, astrophysics and cosmology of theories with submillimeter dimensions and TeV scale quantum gravity”, *Phys. Rev. D* 59 (8): 086004 (1999).
20. Appelquist, T., Cheng, H. C. and Dobrescu, B. A., “Bounds on universal extra dimensions”, *Phys. Rev. D*, 64 (3): 035002-035012 (2001).
21. Geng, C. Q., Hwang, C. W. and Liu, C. C., “Study of rare $B_c^+ \rightarrow D_{d,s}^{(*)+} \ell \bar{\ell}$ decays”, *Phys. Rev. D*, 65 (9): 094037 (2002).
22. Faessler, A., Gutsche, Th., Ivanov, M. A., Körner, J. G. and Lyubovitskij, V. E., “The exclusive rare decays $B \rightarrow K \ell \ell$ and $B_c \rightarrow D(D^*) \ell \ell$ in a relativistic quark model”, *Eur. Phys. J. direct C*, 4 (1): 18-36 (2002).
23. Ebert, D., Faustov, R. N. and Galkin, V. O., “Rare semileptonic decays of B and B_c mesons in the relativistic quark model”, *Phys. Rev. D*, 82 (3): 034032-034056 (2010).
24. Choi, H.-M., “Light-front quark model analysis of the exclusive rare $B_c \rightarrow D_{(s)}(\ell^+ \ell^-, \nu_\ell \bar{\nu}_\ell)$ decays”, *Phys. Rev. D*, 81 (5): 054003-054014 (2010).
25. Wang, T., Liu, T., Zhang, D.-X. and Ma, B.-Q., “ B_c meson rare decays in the light-cone quark model”, *Eur. Phys. J. C*, 71 (9): 1758-1767 (2011)
26. Azizi K. and Khosravi, R., “Analysis of the rare semileptonic $B_c \rightarrow P(D, D_s) \ell^+ \ell^- / \nu \bar{\nu}$ decays within QCD sum rules”, *Phys. Rev. D*, 78 (3): 036005-036022 (2008).
27. Griffiths, D. J., “Introduction to Elementary Particles”, *John Wiley & Sons Inc.*, New York, 11-60 (1987).
28. Peskin, M. E. and Schroeder, D. V., “An Introduction to Quantum Field Theory”, *Addison-Wesley*, USA, 599-615 (1995)

29. Ali, A., Mannel T. and Morozumi, T., “Forward backward asymmetry of dilepton angular distribution in the decay $b \rightarrow s\ell^+\ell^-$ ”, *Phys. Lett. B*, 273 (4): 505-512 (1991).
30. Nakamura, K., *et al.* (Particle Data Group), “Review of particle physics”, *J. Phys. G* 37: 075021 (2010).
31. Randall, L. and Sundrum, R., ”A large mass hierarchy from a small extra dimension”, *Phys. Rev. Lett.*, 83(17): 3370-3373 (1999).
32. Randall, L. and Sundrum, R., ”An alternative to compactification”, *Phys. Rev. Lett.*, 83 (23): 4690-4693 (1999).
33. Kong, K., ”Phenomenology of universal extra dimension”, Ph. D. Thesis, *The Graduate School of University of Florida*, Florida, ABD, 9-18, 103-116 (2006).
34. Riad, S., ”Running of neutrino parameters in extra dimensions”, M. Sc. Thesis, *The School of Engineering Physics, Royal Institute of Technology*, Stockholm, İsveç, 7-22 (2012).
35. Buras, A. J., Spranger, M. and Weiler, A., “The impact of universal extra dimensions on the unitarity triangle and rare K and B decays ”, *Nucl. Phys. B*, 660 (1-2): 225-268 (2003).
36. Buras, A. J., Poschenrieder, A., Spranger, M. and Weiler, A., “The impact of universal extra dimensions on $B \rightarrow X_s\gamma$, $B \rightarrow X_s$ gluon, $B \rightarrow X_s\mu^+\mu^-$, $K_L \rightarrow \pi^0 e^+e^-$ and ε'/ε ”, *Nucl. Phys. B*, 678 (1): 455-490 (2004).
37. Colangelo, P., De Fazio, F., Ferrandes, R. and Pham, T. N., “Exclusive $B \rightarrow K^{(*)}\ell^+\ell^-$, $B \rightarrow K^{(*)}\nu\bar{\nu}$ and $B \rightarrow K^*\gamma$ transitions in a scenario with a single universal extra dimension ”, *Phys. Rev. D*, 73 (11): 115006 (2006).
38. Agashe, K., Deshpande, N. G. and Wu, G. H., “Universal extra dimensions and $b \rightarrow s\gamma$ ”, *Phys. Lett. B*, 511 (3-4): 309-314 (2001).
39. Haisch, U. and Weiler, A., “Bound on minimal universal extra dimensions from $\bar{B} \rightarrow X_s\gamma$ ”, *Phys. Rev D.*, 76 (3): 034014 (2007).
40. Biancofiore, P., Colangelo, P. and Fazio, F., “ $B \rightarrow K\eta'\gamma$ decays in the standard model and in scenarios with universal extra dimensions”, *Phys. Rev. D*, 85 (9): 094012 (2012).
41. Azizi, K., *et. al.*, “Constraint on compactification scale via recently observed baryonic $\Lambda_b \rightarrow \Lambda\ell^+\ell^-$ channel and analysis of the $\Sigma_b \rightarrow \Sigma\ell^+\ell^-$ transition in SM and UED scenario”, *J. High Energy Phys.*, 05: 024- (2012).
42. Yilmaz, U. O., “Study of $B_c \rightarrow D_s^*\ell^+\ell^-$ in a single universal extra dimension”, *Phys. Rev. D*, 85 (11): 115026-115041 (2012).
43. Colangelo, P., De Fazio, F., Ferrandes, R. and Pham, T. N., “Spin effects in rare $B \rightarrow X_s\tau^+\tau^-$ and $B \rightarrow K^{(*)}\tau^+\tau^-$ decays in a single universal extra dimension scenario ”, *Phys. Rev. D*, 74 (11): 115006 (2006).

44. Devidze, G., Liparteliani A. and Meissner, U. G., “ $B_{s,d} \rightarrow \gamma\gamma$ decay in the model with one universal extra dimension”, *Phys. Lett. B*, 634 (1): 59-62 (2006).
45. Mohanta, R. and Giri, A. K., “Study of FCNC-mediated rare B_s decays in a single universal extra dimension scenario”, *Phys. Rev. D*, 75 (3): 035008 (2007).
46. Colangelo, P., De Fazio, F., Ferrandes, R. and Pham, T. N., “FCNC B_s and Λ_b transitions: standard model versus a single universal extra dimension scenario”, *Phys. Rev. D*, 77 (5): 055019 (2008).
47. Saddique, A., Aslam, M. J. and Lu, C. D., “Lepton polarization asymmetry and forwardbackward asymmetry in exclusive $B \rightarrow K_1\tau^+\tau^-$ decay in universal extra dimension scenario”, *Eur. Phys. J. C*, 56 (2): 267-277 (2008).
48. Ahmed, I., Paracha, M. A. and Aslam, M. J., “Exclusive $B \rightarrow K_1\ell^+\ell^-$ decay in model with single universal extra dimension”, *Eur. Phys. J. C*, 54 (4): 591-599 (2008).
49. Bashiry, V. and Zeynali, K., “Exclusive $B \rightarrow \pi\ell^+\ell^-$ and $B \rightarrow \rho\ell^+\ell^-$ decays in the universal extra dimension”, *Phys. Rev. D*, 79 (3): 033006 (2009).
50. Carlucci, M. V., Colangelo P. and De Fazio, F., “Rare B(s) decays to eta and eta-prime final states”, *Phys. Rev. D* 80 (5): 055023 (2009).
51. Li, Y. and Hua, J., “Study of $B_s \rightarrow \phi\ell^+\ell^-$ decay in a single universal extra dimension model”, *Eur. Phys. J. C*, 71: 1764 (2011).
52. Katirci N. and Azizi, K., “B to strange tensor meson transition in a model with one universal extra dimension”, *J. High Energy Phys.*, 07: 043 (2011).
53. Aliev, T. M. and Savci, M., “ $\Lambda_b \rightarrow \Lambda\ell^+\ell^-$ decay in universal extra dimensions”, *Eur. Phys. J. C*, 50 (1): 91-99 (2007).
54. N. Katirci and K. Azizi, “Investigation of the $\Lambda_b \rightarrow \Lambda\ell^+\ell^-$ transition in universal extra dimension using form factors from full QCD”, *J. High Energy Phys.*, 01: 087 (2011).
55. Yilmaz, U. O., “Rare $B_c \rightarrow D_s\ell^+\ell^-$ decay beyond the standard model”, *Phys. Rev. D*, 78 (5): 055004-055012 (2008).
56. Ali, A., Ball, P., Handoko, L. T. and Hiller, G., “Comparative study of the decays $B \rightarrow (K, K^*)\ell^+\ell^-$ in the standard model and supersymmetric theories”, *Phys. Rev. D*, 61 (7): 074024-074043 (2000).
57. Fukae, S., Kim, C. S. and Yoshikawa, T., “Systematic analysis of the lepton polarization asymmetries in the rare B decay $B \rightarrow X_s\tau^+\tau^-$ ”, *Phys. Rev. D*, 61 (7): 074015 (2000).
58. Krüger, F. and Sehgal, L. M., “Lepton polarization in the decays $B \rightarrow X_s\mu^+\mu^-$ and $B \rightarrow X_s\tau^+\tau^-$ ”, *Phys. Lett. B*, 380 (1-2): 199-204 (1996).

APPENDIX A.
INPUT PARAMETERS

$$m_{B_c} = 6.28 \text{ GeV}$$

$$m_{D_s} = 1.968 \text{ GeV}$$

$$m_D = 1.870 \text{ GeV}$$

$$m_b = 4.8 \text{ GeV}$$

$$m_\mu = 0.105 \text{ GeV}$$

$$m_\tau = 1.77 \text{ GeV}$$

$$m_W = 80.40 \text{ GeV}$$

$$m_Z = 91.18 \text{ GeV}$$

$$\sin^2\theta_W = 0.223$$

$$|V_{tb}V_{ts}^*| = 0.041$$

$$|V_{tb}V_{td}^*| = 0.008$$

$$G_F = 1.17 \times 10^{-5} \text{ GeV}^{-2}$$

$$\tau_{B_c} = 0.46 \times 10^{-12} \text{ s}$$

AUTOBIOGRAPHY

Elif DANAPINAR was born in Karabük, Turkey, in 1983. She graduated from Anatolian High School in 2003. She received her B.S degree in physics at Cumhuriyet University in Sivas, Turkey, in 2008. After completing the B.S program, She started her M. Sc. studies on high energy physics at Karabük University in Karabük, Turkey, in 2009.